University of Kentucky
UKnowledge

Theses and Dissertations--Mechanical Engineering

Mechanical Engineering

2018

SCALE MODELS OF ACOUSTIC SCATTERING PROBLEMS INCLUDING BARRIERS AND SOUND ABSORPTION

Nan Zhang
University of Kentucky, zhangnan891020@gmail.com
Author ORCID Identifier:
https://orcid.org/0000-0003-2707-8716
Digital Object Identifier: https://doi.org/10.13023/etd.2018.304

Right click to open a feedback form in a new tab to let us know how this document benefits you.

Recommended Citation

Zhang, Nan, "SCALE MODELS OF ACOUSTIC SCATTERING PROBLEMS INCLUDING BARRIERS AND SOUND ABSORPTION" (2018). *Theses and Dissertations--Mechanical Engineering*. 119.
https://uknowledge.uky.edu/me_etds/119

This Master's Thesis is brought to you for free and open access by the Mechanical Engineering at UKnowledge. It has been accepted for inclusion in Theses and Dissertations--Mechanical Engineering by an authorized administrator of UKnowledge. For more information, please contact UKnowledge@lsv.uky.edu.

STUDENT AGREEMENT:

I represent that my thesis or dissertation and abstract are my original work. Proper attribution has been given to all outside sources. I understand that I am solely responsible for obtaining any needed copyright permissions. I have obtained needed written permission statement(s) from the owner(s) of each third-party copyrighted matter to be included in my work, allowing electronic distribution (if such use is not permitted by the fair use doctrine) which will be submitted to UKnowledge as Additional File.

I hereby grant to The University of Kentucky and its agents the irrevocable, non-exclusive, and royalty-free license to archive and make accessible my work in whole or in part in all forms of media, now or hereafter known. I agree that the document mentioned above may be made available immediately for worldwide access unless an embargo applies.

I retain all other ownership rights to the copyright of my work. I also retain the right to use in future works (such as articles or books) all or part of my work. I understand that I am free to register the copyright to my work.

REVIEW, APPROVAL AND ACCEPTANCE

The document mentioned above has been reviewed and accepted by the student's advisor, on behalf of the advisory committee, and by the Director of Graduate Studies (DGS), on behalf of the program; we verify that this is the final, approved version of the student's thesis including all changes required by the advisory committee. The undersigned agree to abide by the statements above.

Nan Zhang, Student

Dr. David W. Herrin, Major Professor

Dr. Alexandre Martin, Director of Graduate Studies

SCALE MODELS OF ACOUSTIC SCATTERING PROBLEMS INCLUDING BARRIERS AND SOUND ABSORPTION

THESIS

A Thesis submitted in partial fulfillment of the
requirements for the degree of Master of Science
in Mechanical Engineering in the College of Engineering
at the University of Kentucky

By

Nan Zhang

Lexington, Kentucky

Director: Dr. David W. Herrin, Professor of Mechanical Engineering

Lexington, Kentucky

2018

Copyright © Nan Zhang 2018

ABSTRACT OF THESIS

SCALE MODELS OF ACOUSTIC SCATTERING PROBLEMS INCLUDING BARRIERS AND SOUND ABSORPTION

Scale modeling has been commonly used for architectural acoustics but use in other noise control areas is nominal. Acoustic scale modeling theory is first reviewed and then feasibility for small-scale applications, such as is common in the electronics industry, is investigated. Three application cases are used to examine the viability. In the first example, a scale model is used to determine the insertion loss of a rectangular barrier. In the second example, the transmission loss through parallel tubes drilled through a cylinder is measured and results are compared to a 2.85 times scale model with good agreement. The third example is a rectangular cuboid with a smaller cylindrical well bored into it. A point source is placed above the cuboid. The transfer function was measured between positions on the top of the cylinder and inside of the cylindrical well. Treatments were then applied sequentially including a cylindrical barrier around the well, a membrane cover over the opening, and a layer of sound absorption over the well. Results are compared between the full scale and a 5.7 times scale model and correlation between the two is satisfactory.

KEYWORDS: Scale Modeling, Acoustic Scattering, Noise Reduction, Transfer Function, Finite Element Method.

Nan Zhang

Student's Signature

25th July, 2018

SCALE MODELS OF ACOUSTIC SCATTERING PROBLEMS INCLUDING BARRIERS AND SOUND ABSORPTION

By

Nan Zhang

Dr. Alexandre Martin
Director of Graduate Studies

Dr. David W. Herrin
Director of Thesis

25th July, 2018
Date

To my family

ACKNOWLEDGEMENTS

Firstly, I would like to express my gratitude to my advisor Professor David Herrin for his continuous guidance and support during my master study at University of Kentucky. His fund of knowledge changed my thinking perspective as an advisor. His insight broadened my life horizon as a mentor. My appreciation is also sent to Professor Tingwen Wu for his help and advice on my research work. In addition, I would also like to give my thanks to Dr. John Baker for his valuable comments and recommendations on my thesis work.

I have enjoyed my life and study so much at university of Kentucky. It's been a precious experience and memory on my life road. I want to give thanks to all my fellows and friends in Vibro-Acoustic Lab, Jonathon Chen, Gong Cheng, Huangxing Chen, Keyu Chen, Weiyun Liu, Kangping Ruan, Shujian He, Conner Campbell, Yitian Zhang, Wanlu Li, Peng Wang, Jundong Li, Caoyang Li, Ruimeng Wu, Xin Hua, Jinghao Liu, Limin Zhou, Rui He, Xin Yan, Hao Zhou and Shishuo Sun, for all the fun we have had in the past several years.

Last but the most important, I would like to give my sincere thankfulness to my Lord and my family. Ephesians 1:8 the grace that he lavished on us with all wisdom and understanding. My dear mother, Guiqin Xu, who sacrifices her whole life to raise me up and taught me what person I should be. My great father, Hongzhi, Zhang, who always supports me whenever I need for what I do right, sets himself as a role model to show me how important the hardworking and integrity can change my career and life. My beloved fiancée, Jie Zhang, who cooks for me on a daily basis, holds my hands walking through with me for all the ups and downs

I have been through. My lovely sister, Ning Ning, who brings all the laughter and enthusiasm into my life, which fills my life with full of sunshine. They make me be the best person I could ever be. I would never become the person I am now without them. Thank you, my family. I love you all.

TABLE OF CONTENTS

ACKNOWLEDGEMENTS iii

LIST OF TABLES vii

LIST OF FIGURES viii

CHAPTER 1 INTRODUCTION 1

1.1 Introduction 1

1.2 Objectives 4

1.3 Outlines 5

CHAPTER 2 BACKGROUND 6

2.1 Background on Scale Modeling 6

2.2 Background on Acoustic Theory 9

2.2.1 Analytical Approach to Determine Barrier Insertion Loss 9

2.2.2 One Dimensional Wave Equation 12

2.2.3 Acoustic Source Modeling 13

2.2.4 Acoustic Transmission Loss 15

2.3 Background on Acoustic Material 17

2.3.1 Limp Panel Theory 17

2.3.2 Modes of Circular Panel 20

2.3.3 Definition and Determination of Flow Resistivity 20

CHAPTER 3 SCALE MODELING RULES FOR VIBRO-ACOUSTICS 24

3.1 Introduction 24

3.2 Review of Scale Modeling Rules for Acoustics 24

3.2.1 Acoustic Wave Propagation 24

3.2.2 Sound Transmission through a Limp Panel 26

3.2.3 Sound Propagation through a Sound Absorption Material 27
3.3 Summary 29
CHAPTER 4 EXAMPLE – BARRIER 30
4.1 Barrier Insertion Loss 30
4.2 Summary 34
CHAPTER 5 EXAMPLE – PARALLEL TUBES 35
5.1 Transmission Loss through Parallel Tubes 35
5.2 Summary 38
CHAPTER 6 EXAMPLE – CUBOID WITH CYLINDRICAL WELL 39
6.1 Introduction 39
6.2 Test Description 40
6.3 Modification Cases 44
6.3.1 Cylindrical Barrier Treatment 44
6.3.2 Membrane Treatment 47
6.3.3 Absorption Treatment 48
6.4 Summary 51
CHAPTER 7 CONCLUSIONS AND FUTURE RECOMMENDATIONS 52
7.1 Conclusions 52
7.2 Recommendations for Future Work 54
REFERENCES 55
VITA 61

LIST OF TABLES

Table 2.1 Values of λmn for a clamped and circular plate of radius $r0$ (Nilsson and Liu, 2012)..... 20

Table 2.2 University of Kentucky airflow apparatus measured flow resistance and resistivity for polyurethane foam. 23

LIST OF FIGURES

Figure 2.1 Geometry of a simple barrier (Long, 2014) 9

Figure 2.2 Path length difference for a simple barrier (Long, 2014) 10

Figure 2.3 Possible sound paths around a finite barrier (Long, 2014)..... 11

Figure 2.4 Point source at University of Kentucky Vibro-Acoustic Lab..... 14

Figure 2.5 Point source directivity calibration..... 15

Figure 2.6 Definition of muffler transmission loss..... 15

Figure 2.7 Schematic of Transmission loss test setup 16

Figure 2.8 Schematic of acoustic wave decomposition and TL test configurations..... 17

Figure 2.9 Sound transmission through a thin plate of thickness t..... 18

Figure 2.10 Schematic of measuring flow resistance (ASTM, 2003)..... 21

Figure 2.11 Flow resistance test rig of University of Kentucky 22

Figure 4.1 Photograph of full-scale and scaled barriers..... 30

Figure 4.2 Schematic showing of the barrier insertion loss test 31

Figure 4.3 Measurement setup for full barrier and its scale model..... 31

Figure 4.4 FEM model of the barrier 32

Figure 4.5 Insertion loss comparison for barrier between full and scale model…….....33

Figure 4.6 Analytical, FEM and test results comparison for barrier 34

Figure 5.1 Transmission loss test setup for an array of parallel tubes 35

Figure 5.2 Transmission loss results comparison 37

Figure 6.1 Photograph of full structure and its scale model (left). Schematic dimensions for the full model (right)..... 41

Figure 6.2 Transfer function measurement setup for full model 41

Figure 6.3 Transfer function measurement setup for scale model 42

Figure 6.4 Finite and boundary element models 42

Figure 6.5 Transfer function comparison showing unscaled, 5.7X scale, and FEM and BEM simulation. 43

Figure 6.6 Photograph of the cylindrical barrier treatment for full structure (left) with the schematic dimensional view..... 44

Figure 6.7 Schematic view of the FEA model for cylindrical barrier treatment 45

Figure 6.8 Transfer function comparisons between measured, and FEM and BEM simulation..... 45

Figure 6.9 Photograph of the membrane treatment for scale model structure (left) with the schematic and dimensions (right)..... 47

Figure 6.10 Transfer function comparison between baseline and membrane treated. Scale model results are also included 48

Figure 6.11 Photograph of the absorption treatment for scale model structure (left) with the schematic dimensional view..... 49

Figure 6.12 Schematic view of the FEA model for absorption treatment..... 50

Figure 6.13 FEM and experiment results of the transfer function comparison for the absorption treatment with scale model 50

CHAPTER 1 INTRODUCTION

1.1 Introduction

Scale modeling approaches are commonly used to investigate problems in a number of engineering disciplines. They have been primarily used to reduce the cost of expensive full-scale prototypes. Though they are less relied on now than in the past because of advances in numerical simulation, they still serve as a helpful model validation tool. Moreover, some problems are difficult to model using simulation, and scale models are still the most appropriate investigative technique.

The primary issue in developing a scale model is to adequately represent the physics of the full-scale case so that the scale model is useful. Often, some concessions must be made and the limitations of the scale model must be understood.

In most cases, a much smaller scale model is developed for the real structure. For example, the structural dynamics of a twin turbine-generator set was investigated using a 1/8 times scale model (Bannister, 1968 and Bannister, 1975), small models of auditoriums have been developed to investigate the acoustics (Jordan, 1970; Jordan, 1975; Rindel, 2011), and scale models are frequently used to investigate the fluid dynamics around airfoils (Oerlemans, 2004). Though scale models are not without expense, the advent of 3D printing has greatly reduced the effort to produce scale models depending on the application.

Though perhaps less frequently used in engineering applications, scale models may also be used to investigate phenomenon on geometries that are too

small to instrument. In which case, the scale model will be several times greater in size than the real world geometry. Once again, 3D printing can play a role in constructing appropriate scale models with little manual effort.

This thesis looks at the utility of using scale models for acoustic applications. In all prior research to the author's knowledge, the geometry has been reduced in size. This is typical of architectural acoustics (i.e., theaters, auditoriums, and similar structures) and transportation industry (i.e., highway and train barrier) applications. Full-scale prototypes of this size are not feasible and so a reduced scale prototype is the only recourse. Scale models for comparably smaller industrial applications are also feasible, but are less common because numerical simulation has been preferred and full-scale prototypes developed and tested extensively.

Acoustic concerns in performance spaces are unique with an overriding goal of insuring that the audience experience is favorable. In transportation and industrial applications, the goal is to boost the amount of noise abatement.

A growing acoustics concern is that of handheld or other small electronics devices such as cell phones, tablets, laptops, and small speakers. In these cases, objectives are varied and often involve minimizing the amount of sound attenuation. This is the opposite of most transportation and industry applications. For example, the microphone of a smart-phone resides in a well and is covered by an impermeable membrane. Smart-phone manufactures are naturally concerned about the amount of acoustic attenuation through the membrane. Attenuation in select frequency bands is desirable but sound transmission is desirable at most

frequencies. Another example is the air flow path for cooling of laptop internals. The geometry and length of the path can greatly affect the sound level when the fan is running. In both of these examples, it is desirable to measure the sound field to better understand the acoustics. However, the acoustic space is difficult to instrument and measure due to the small size of the geometry.

In these examples and others, scale models would appear to be an ideal way to explore the acoustics. Rather than scale the geometry down, the geometry can be scaled up so that it can be easily instrumented. 3D printing can be used to expedite scale model creation.

In this work, the scaling laws for acoustics are reviewed and then are applied to several examples. The first example is a rectangular barrier. The primary purpose of this example was to gain confidence in the measurement and simulation procedures. The second example considered is sound transmission through a collection of parallel tubes. The transmission loss ,which is the most common metric for characterizing sound attenuation, is measured on both the unscaled and a 2.85 times scaled model.

When the geometry is small, thermo-viscous effects may become important. The aforementioned study examines the potential differences between scaled and unscaled models due to these effects.

Following the first two examples, a more novel case was studied that is more typical of the small geometries in electronics equipment. A 15 cm tall rectangular cuboid with a 2 cm diameter bore is considered. The size of the geometry is about the smallest size that can be instrumented using measurement

grade microphones. Measurements were also made on approximately a 5.7 times scale model. Barriers, a membrane cover, and a resistive cover are also considered to demonstrate that the procedure can be used for more complicated applications.

For completeness, acoustic finite element models are created for each of the examples. Results are then compared between the original, scaled model, and finite element simulation. Several recommendations are made based on the results.

1.2 Objectives

The objectives of this research are to:

1) Review the scaling laws for acoustic waves, limp panels, and resistive sound absorptive material.
2) Validate the scaling laws on examples that are relevant to the real world applications.
3) Identify some of the possible limitations of scale models for acoustics applications.
4) Demonstrate that the acoustic scale models correlate well with numerical simulation.

1.3 Outlines

The organization of this thesis is as follows.

Chapter 1 introduces the topic and the need for further research on scale models especially for small-scale applications like those commonly encountered in the electronics industry. Chapter 2 reviews the literature on scale models and surveys the acoustic theory required for understanding the test cases. Chapter 3 introduces the scaling laws, and scaling rules are developed for vibro-acoustic uses. Chapter 4 illustrates the scaling laws on a rectangular barrier. Chapter 5 applies the scaling laws to find the attenuation through small parallel tubes. Chapter 6 applies the scaling laws to a cylindrical well successively treated with a barrier, a membrane cover, and a sound absorptive cover. In chapter 7, the research is summarized and future work is recommended.

Copyright © Nan Zhang 2018

CHAPTER 2 BACKGROUND

2.1 Background on Scale Modeling

Scale modeling has been widely used in the past in many engineering fields to investigate critical design issues especially when computer simulation of the physical phenomenon is difficult. Testing on a full scale prototype sometimes requires large and expensive test facilities. In the field of acoustics and noise control, this is certainly the case for problems involving large spaces or large machinery. Hence, scale modeling approaches are advantageous particularly if the model is easy to develop.

Not surprisingly, scale models have been used to explore and solve problems in the architectural, building, and transportation industries. In formative work, Jordan (1970, 1975) developed scale models for auditoriums to examine the acoustics. In rooms and other large spaces, the sound reaching an observer is a combination of that from the source, called the direct field, and coming from reflections off the walls, termed the reverberant field. If the reflected sound (i.e., the reverberant field) is dominant, speech intelligibility will suffer. The amount of reflected sound can be reduced by adding sound absorptive linings to the walls or adding sound absorptive seats. The standard method for determining the amount of reverberation in a room is to introduce broadband sound in the room using a loudspeaker and then switch the speaker off. Reverberation time is defined as the amount of time until the sound decreases by 60 dB and is ideally around 2 seconds for most auditoriums. Jordan used scale models in an effort to determine the

reverberation time. In the similar work, Day and White (1969) used a scale model to look at the sound field inside an office building. The scale model was primarily for the purpose of better understanding the sound field. Jeon et al. (2009) explored the effect of different sound absorbing surfaces in auditoriums and noted that the differences in the diffuseness of a sound field between the full scale and scale models can lead to differences between the two.

Scale models have been especially valuable for examining the attenuation of barriers. For example, Ivey and Russell (1977) treated buildings as wide sound barriers. They used a point acoustic source and measured the sound pressure on the opposite side. Results were compared to theoretical results based on the Fresnel number, the difference in distance between the most direct path over the barrier and the distance between source and receiver. Wadsworth and Chambers (2000) investigated the attenuation of impulsive noise (i.e. impact noise) due to single and double knife-edge (i.e., thin) barriers and a wide barrier. Busch et al. (2003) measured the insertion loss of highway noise barriers and berms using scale models. As in the other studies, they explored the effect of barrier geometry. Moreover, the sound absorption of the barrier (i.e., soil in the case of berms) was considered in the study.

After these early studies, scale modeling was largely abandoned for acoustic applications with the advent of numerical simulation. The time and effort involved in developing a scale model was prohibitive except for a few specialized applications. However, there is renewed interest in scale modeling acoustical spaces with the advent of 3D printing. In recent work, Brown (2016) has used 3D-

print models to develop scale models for architectural acoustics applications overcoming the primary difficulties of model construction and cost. Brown investigated the acoustics of a reverberation room, a specialized room for making sound power and absorption coefficient measurements, using a 1/10th scale model.

In recent work at the University of Kentucky, scale models have been combined with panel contribution analysis (PCA) to determine the sound emitted from vibrating machinery. PCA is an approach where a radiating object is discretized into a set of patches. The acoustic volume velocity from each patch is measured on the running machine. Volume velocities are then multiplied by acoustic transfer functions which are the ratio of the sound pressure at a receiver to the acoustic volume velocity of a patch. Scale models were used to determine the acoustic transfer functions. Applications included a structure excited by shaker (Liu et al., 2011), a small power generator set (Cheng and Herrin, 2015), mining equipment (Herrin et al., 2017), and air handlers in a bakery (Cheng and Herrin, 2018).

Scale modeling is markedly far more difficult if sound absorption is included. In most prior research (Jeon et al., 2009; Busch et al., 2003), the sound absorption was scaled with the aim to produce a similar sound absorption coefficient at different frequencies. However, matching the sound absorption does not necessarily insure that the acoustics are the same. Rather, correlation will be much better if the normal incident impedance is the same since the phase of the reflected wave is also considered. Horoshenkov and Hothersall (1996) suggested

a systematic approach for developing scaled models of sound absorbers so that the normal incident impedance was scaled properly. The method developed is also usable for thick absorbers.

The scaling laws will be described in detail in later chapters. For purely acoustic applications, scaling laws for acoustic waves and for characterizing sound absorptive materials are sufficient for most architectural applications and also for panel contribution analysis. In addition, appropriate scaling of the sound absorption coefficient should be acceptable for most engineering needs. Unfortunately, exact scaling of the sound absorption necessitates scaling at the micro-structure level which is difficult in practice.

2.2 Background on Acoustic Theory

In the sections that follow, basic acoustic theory that is relevant to the research is summarized.

2.2.1 Analytical Approach to Determine Barrier Insertion Loss

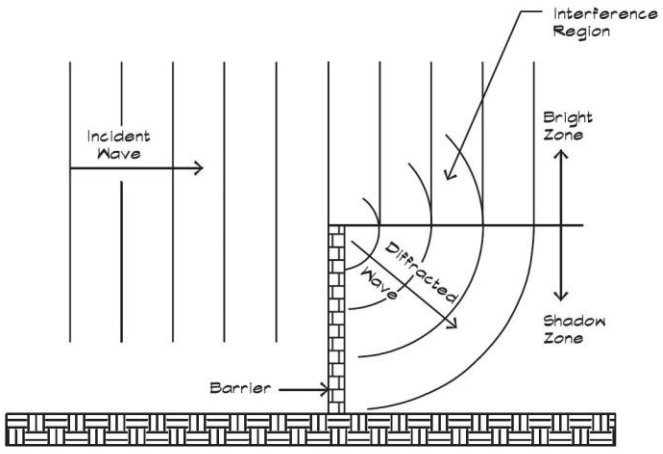

Figure 2.1 Geometry of a simple barrier (Long, 2014)

Barriers are commonly used to reduce highway and train noise. Sound is reflected by the barrier back towards the source. However, sound will diffract around a barrier as shown in Figure 2.1 especially at low frequencies. The region behind the barrier is commonly referred to as the shadow zone.

Simple equations for barriers are described by Long (2014) following the work of Maekawa (1968). Figure 2.2 shows a rigid, semi-infinite barrier placed between a source and an observer.

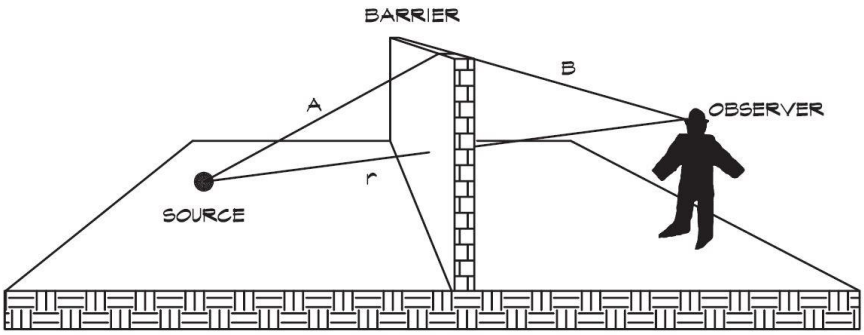

Figure 2.2 Path length difference for a simple barrier (Long, 2014)

The Fresnel number is defined as the difference between the shortest propagation path $(A + B)$ and the distance between the source and observer (r) divided by one half of an acoustic wavelength(λ). It can be expressed as

$$N_i = \pm\frac{2}{\lambda}(A_i + B_i - r) \tag{2.1}$$

where the sign is positive in the shadow zone and negative in the bright zone. The barrier sound attenuation $\triangle L_b$ in dB for a point source with path i can be approximated as

$$\Delta L_b = 20 \log \left(\frac{\sqrt{2\pi N_i}}{\tanh \sqrt{2\pi N_i}} + K_b \right) \tag{2.2}$$

where N_i is the maximum Fresnel number for path i over the barrier, and K_b is the barrier constant which is 5 dB for a wall and 8 dB for a berm. For a simple semi-infinite barrier, only one path where the sound wave is diffracted over the top edge of the barrier is taken into account. This also assumes that the ground reflection path is ignored.

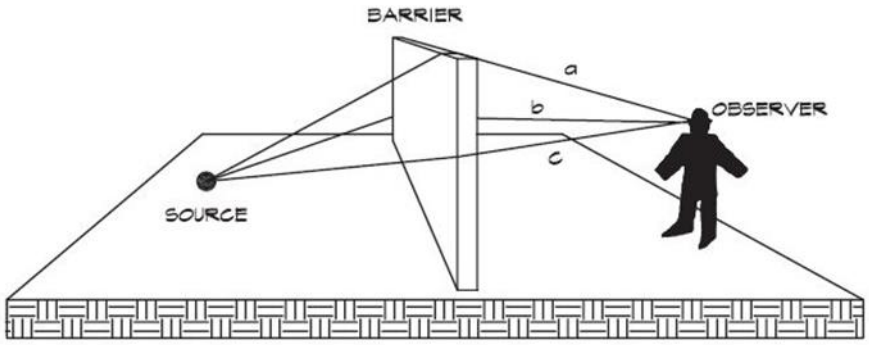

Figure 2.3 Possible sound paths around a finite barrier (Long, 2014)

If barriers are finite in length, not only the sound travelling over the top (path a) but also around the sides (paths b and c) is of importance. An example is shown in Figure 2.3. Barrier attenuation is calculated for each path using Eq. (2.2). The total attenuation or noise reduction is determined using

$$NR = 10 \log_{10} \sum_{1}^{i} 10^{-(\Delta L_{bi}/10)} \tag{2.3}$$

where ΔL_{bi} is the noise reduction for each path individually.

2.2.2 One Dimensional Wave Equation

The one-dimensional wave acoustic wave equation is expressed as

$$\frac{d^2p(x,t)}{dx^2} = \frac{1}{c}\frac{d^2p(x,t)}{dt^2} \tag{2.4}$$

where P is the sound pressure, x is the position, t is the time, and c is the speed of sound. Assuming harmonic behavior, the sound pressure can be expressed as the sum of a propagating and reflected wave. The sound pressure $p(x,t)$ can be written as

$$p(x,t) = P_+ e^{i(\omega t - kx)} + P_- e^{i(\omega t + kx)} \tag{2.5}$$

where P_+ and P_- are the propagating and reflected waves respectively and k is the wavenumber defined as the ratio of the angular frequency (ω) to the speed of sound (c). The acoustic particle velocity can be related to the equation of motion using the expression

$$\rho_0 \dot{u}(x,t) = -\frac{dp(x,t)}{dx} \tag{2.6}$$

It follows that the particle velocity can be expressed as

$$u(x,t) = \frac{P_+}{\rho_0 c} e^{i(\omega t - kx)} - \frac{P_-}{\rho_0 c} e^{i(\omega t + kx)} \tag{2.7}$$

2.2.3 Acoustic Source Modeling

A monopole (i.e., an ideal point source) is the simplest acoustic source. The geometrical dimension is assumed to be negligible. If Helmholtz equation is solved in spherical coordinates, the sound pressure can be expressed as

$$P(r,t) = \frac{A}{r} e^{i(\omega t - kr)} \tag{2.8}$$

where k is the wave number, r is the distance bewtween monopole center and receiver position, and A is the amplitude of sound pressure. The amplitude of the monopole is often expressed as a volume velocity. It can be related to the sound pressure amplitude as

$$Q_0 = \frac{4\pi A}{i\rho_0 ck} \tag{2.9}$$

where ρ_0 is defined as the density, c as the speed of sound, and k as the wavenumber. By inserting the Eq. (2.9) into Eq. (2.8), a monopole can be expressed as

$$P_m = \frac{i\rho_0 \omega Q_0}{4\pi r} e^{-ikr} \tag{2.10}$$

A source which approximates the theoretical monopole is shown in Figure 2.4. This source was used for all measurements in this thesis. A shop air supply is directed into a metal tube. This tube is then attached to a whiffle ball with holes as shown. The top of the ball is covered by duct tape. The flow into the ball creates an aeroacoustic source that is nearly omni-directional at most frequencies.

Liu et al. (2011) validated the source using ISO 140-4 (ISO, 1998) and ISO 3382 (ISO, 1997). The source falls short of the standard at very low frequencies but is acceptable for the purposes of this research.

Figure 2.4 Point source at University of Kentucky Vibro-Acoustic Lab

The procedure to calibrate the source is to place a microphone at 30 cm. Assuming that the source acts as a point source, the sound pressure level can be measured and the source strength determined using Eq. (2.10). In this research, 3 microphones were used to insure that the source was behaving appropriately as a monopole. A photo of the calibration procedure is shown in Figure 2.5.

Figure 2.5 Point source directivity calibration

2.2.4 Acoustic Transmission Loss

Transmission loss is the most common metric for assessing the performance of mufflers. A muffler is illustrated in Figure 2.6. The incident, reflected, and transmitted wave amplitudes are indicated.

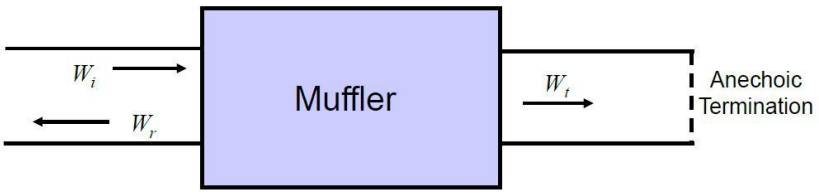

Figure 2.6 Definition of muffler transmission loss

Transmission loss is defined as the difference in dB between the incident and transmitted powers assuming an anechoic termination. Hence, it can be expressed as

$$TL(dB) = 10 \log_{10} \frac{W_i}{W_t} \tag{2.11}$$

where W_i is the incident wave amplitude and W_t is the transmitted wave amplitude.

The standard test for measuring transmission loss is detailed in ASTM E2611 (ASTM, 2009). The measurement is performed by placing the test element between two impedance tubes as indicated in Figure 2.7. A loudspeaker is placed on one side. Two microphones are mounted on each side of the element under test. A multi-channel data acquisition system is used to collect data. The acoustic load is varied twice by changing the termination. Best results are obtained if one load is absorbing and the other is reflective. Transfer functions are measured between the microphones.

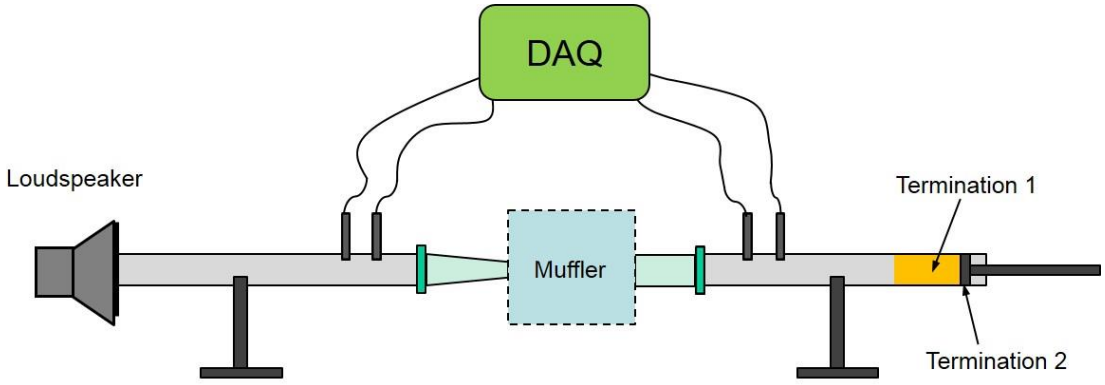

Figure 2.7 Schematic of Transmission loss test setup

Using the algorithms detailed in ASTM E2611, the measured transfer function information can be used to determine the transfer matrix for the muffler. The transfer matrix relates the sound pressure and particle velocity on one side to that on the other. The transfer matrix is expressed as

$$T = \begin{bmatrix} T_{11} & T_{12} \\ T_{21} & T_{22} \end{bmatrix} \tag{2.12}$$

where T_{11}, T_{12}, T_{21} and T_{22} are the transfer matrix terms.

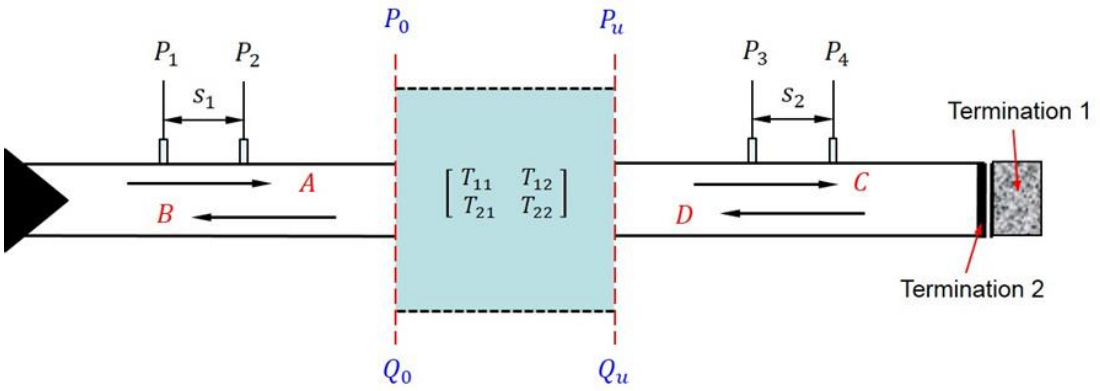

Figure 2.8 Schematic of acoustic wave decomposition and TL test configurations

Transmission loss of the muffler can be determined using

$$TL = 20\ \log_{10}\left|\frac{1}{2}\left(T_{11} + \frac{S}{\rho c}T_{12} + \frac{\rho c}{S}T_{21} + T_{22}\right)\right| \tag{2.13}$$

where S is the cross-sectional area of the duct.

2.3 Background on Acoustic Material

2.3.1 Limp Panel Theory

Limp panel theory can be used to assess the amount of sound transmission through a wall or membrane. The theory is most appropriate after the first several panel modes. Figure 2.9 shows a schematic of a limp panel with an incident wave having complex amplitude A striking it. Part of the energy is reflected (with complex amplitude B) while the remainder goes into the panel and vibrates it as a

rigid body. Bending waves in the panel are not considered. Only the mass of the panel is considered, and stiffness and damping effects are ignored. As the panel vibrates with velocity u_p, sound is radiated back towards the source (complex amplitude C') and transmitted (complex amplitude C).

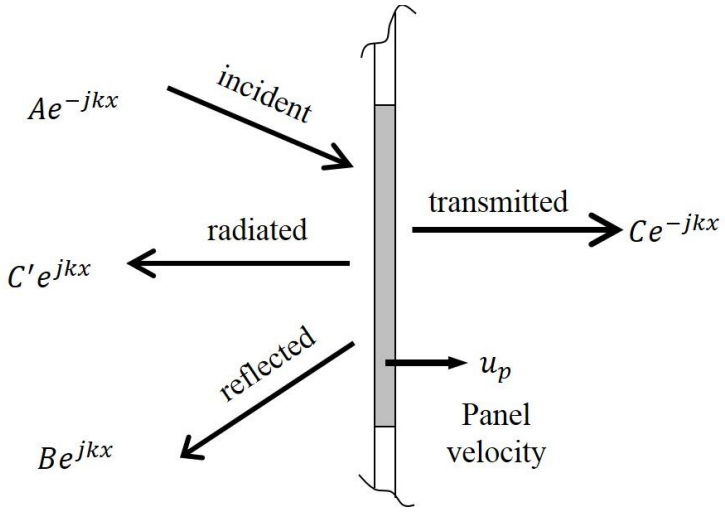

Figure 2.9 Sound transmission through a thin plate of thickness t

Using Newton's 2nd Law, the acceleration of the panel can be expressed in terms of the complex wave amplitudes. This is written as

$$m\dot{u}_p = S(A + B + C' - C) \tag{2.14}$$

where m is the panel mass, and S is the panel area. A, B, C' and C are the amplitude of the incident, reflected, radiated and transmitted wave, respectively. Notice that C' and C are out of phase with one another. If the sound absorption of the panel is assumed to be negligible, $A = B$. Assuming mass continuity, the particle velocities of the waves (u_A, u_b, and $u_{c'}$) can be expressed as a function of the panel motion (u_p). This is expressed mathematically as

$$u_p = u_A + u_B + u_{c'} \tag{2.15}$$

The panel motion can then be expressed in terms of the complex wave amplitudes as

$$u_p = (A - B - C')/\rho_0 c \tag{2.16}$$

Combining Equations (2.14) and (2.16), the ratio between the transmitted (C) and incident (A) wave amplitudes can be expressed as

$$C/A = \frac{1}{1 + j\omega m/2\rho_0 cS} \tag{2.17}$$

The transmission coefficient (τ) is defined as the ratio of the transmitted to incident power. The panel transmission loss is then expressed as

$$TL = 10 \log_{10} \frac{1}{\tau} \tag{2.18}$$

where the transmission coefficient is given as

$$\tau = \frac{I_t}{I_i} = \frac{|C|^2/\rho_0 c}{|A|^2/\rho_0 c} = \frac{1}{1 + (\omega m/2\rho_0 cS)^2} \tag{2.19}$$

Note that the transmission coefficient is not dependent on the stiffness or damping of the plate.

2.3.2 Modes of Circular Panel

As noted in the prior section, the transmission loss above the first several panel modes is primarily a function of the panel mass. At lower frequencies, panel modes manifest themselves as a trough in the response. For a circular panel with a clamped edge, the panel mode natural frequencies f_{mn} can be determined using

$$f_{mn} = \frac{1}{2\pi}\left(\frac{\lambda_{mn}}{r_0}\right)^2 \sqrt{\frac{D_0}{\mu}} \tag{2.20}$$

where μ is the mass per unit area of the plate, D_0 is the bending stiffness, r_0 is the radius of the plate, and λ_{mn} is the parameter which can be referenced from Table 2.1 (Nilsson and Liu, 2012).

Table 2.1 Values of λ_{mn} for a clamped and circular plate of radius r_0 (Nilsson and Liu, 2012)

m	$n = 1$	$n = 2$	$n = 3$	$n = 4$
0	3.196	6.306	9.439	12.575
1	4.611	7.799	10.958	14.109
2	5.906	9.197	12.402	15.579
3	7.144	10.536	13.795	17.005

2.3.3 Definition and Determination of Flow Resistivity

Flow resistance (r_s) is defined as the ratio of steady airflow pressure difference (ΔP) across a specimen material divided by the airflow velocity (u) through it. It is defined as

$$r_s = \frac{\Delta P}{u} \tag{2.21}$$

Flow resistivity (σ) is defined as the flow resistance divided by the thickness (t) of the sound absorber. It follows that the flow resistivity can be expressed as

$$\sigma = \frac{r_s}{t} \tag{2.22}$$

Flow resistance is measured using the testing procedure described in ASTM C522 (ASTM, 2003). A schematic showing the test apparatus is shown in Figure 2.10. Air flow is forced through a porous material sample via a blower or other mechanical device and the pressure drop across the sample is measure using a manometer.

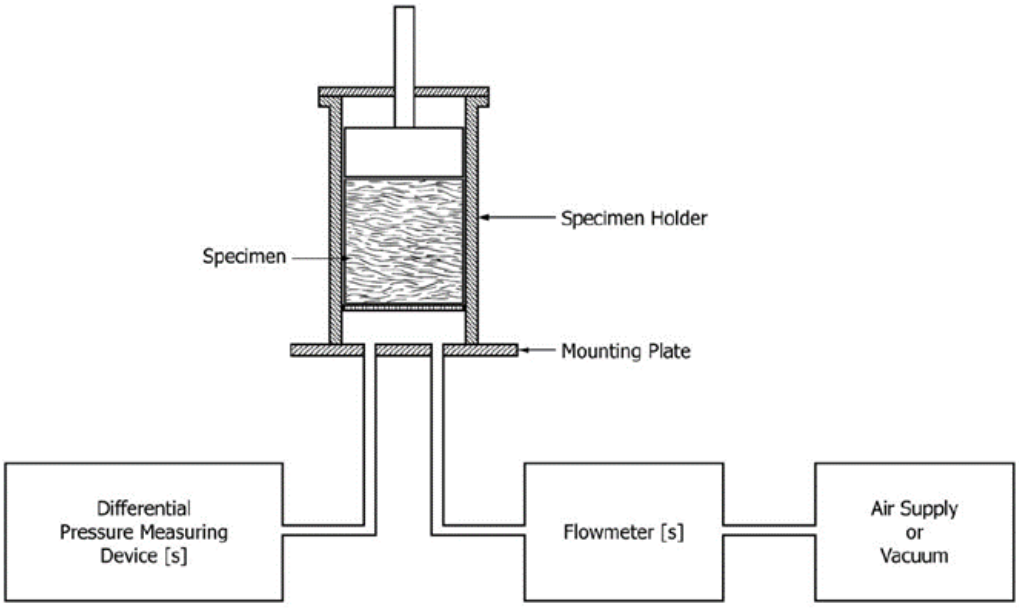

Figure 2.10 Schematic of measuring flow resistance (ASTM, 2003)

A photograph of the University of Kentucky rig is shown in Figure 2.11 with parts identified. The rig incorporates a fan to generate flow, a flow meter to measure the flow velocity, and a manometer to measure the pressure drop. Table 2.2 lists several flow resistances and flow resistivities for open-cell polyurethane foam as it is compressed. Notice that the values for flow resistance are roughly on the same order of magnitude as the material is compressed.

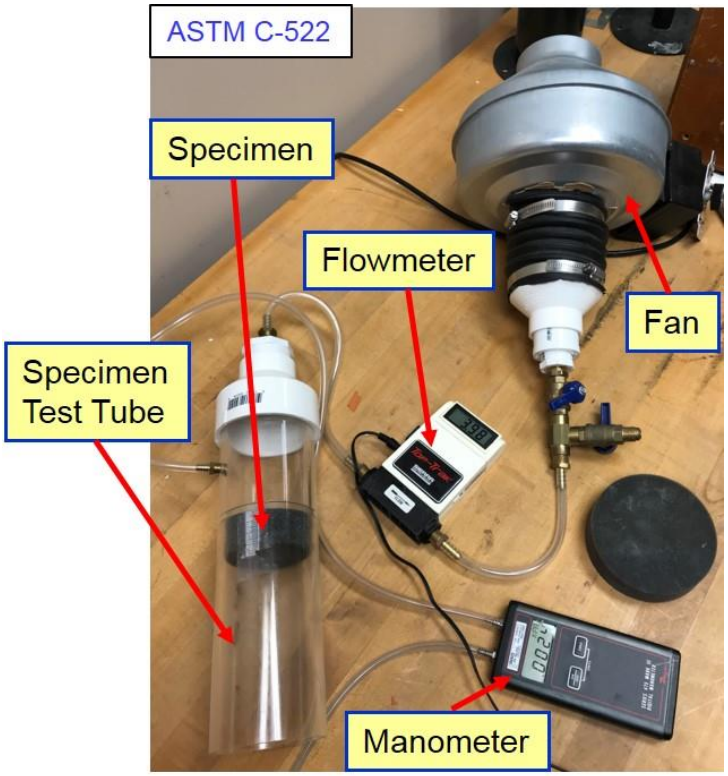

Figure 2.11 Flow resistance test rig of University of Kentucky

Table 2.2 University of Kentucky airflow apparatus measured flow resistance and resistivity for polyurethane foam.

	$t = 86.36\ mm$	$t = 15.88\ mm$	$t = 13.23\ mm$	$t = 10.59\ mm$
Type	Original	Compressed	Compressed	Compressed
r_s (rayls)	338	366	388	436
σ (rayls/m)	4011	23058	29348	41243

Copyright © Nan Zhang 2018

CHAPTER 3 SCALE MODELING RULES FOR VIBRO-ACOUSTICS

3.1 Introduction

Emori and Schuring (1997) detailed the scaling laws for architectural acoustics including acoustic spaces and porous materials. Saito and Kuwana (2017) have also reviewed the scaling equations for acoustics. The sections which follow review the scaling laws and introduce a simple scaling laws for membranes and sound absorbing linings.

3.2 Review of Scale Modeling Rules for Acoustics

3.2.1 Acoustic Wave Propagation

Scale modeling laws for acoustic wave propagation is briefly derived following the method of Emori and Schuring (1997). In a simplified sense, the equation of motion in a fluid can be expressed as

$$F = ma \tag{3.1}$$

where F is force, m is mass, and a is acceleration. Force can be expressed in terms of sound pressure (p) and area or length squared (l^2) as

$$F = pl^2 \tag{3.2}$$

Mass can be expressed as

$$m = \rho l^3 \tag{3.3}$$

where ρ is the mass density. Acceleration is length divided by time squared or

$$a = f^2 l \tag{3.4}$$

where f is frequency assuming harmonic sources. By inserting Equation (3.2), (3.3), and (3.4) into (3.1) and solving for sound pressure, the first Pi number is arrived at and can be expressed as

$$\Pi_A = \frac{p}{\rho f^2 l^2} \tag{3.5}$$

Assuming viscous losses are neglected, the adiabatic equation of state relating the sound pressure to the volumetric strain can be expressed as

$$p = -\rho c^2 \frac{\Delta V}{V} \tag{3.6}$$

where $\Delta V/V$ is the volumetric strain. It follows that the second Pi number can be written as

$$\Pi_B = \frac{p}{\rho c^2} \tag{3.7}$$

Combining Equations (3.5) and (3.7) by eliminating the sound pressure, the Pi number for sound transmission can be arrived at and expressed as

$$\Pi_1 = \frac{\Pi_A}{\Pi_B} = \frac{f^2 l^2}{c^2} \tag{3.8}$$

If air is assumed to be the same fluid medium in both full and scale models, the relationship between the models can be expressed as

$$f_1 l_1 = f_2 l_2 \tag{3.9}$$

Thus, the frequencies between the full and scale model are inversely proportional to their geometrical dimensions.

3.2.2 Sound Transmission through a Limp Panel

The transmission coefficient (τ) for a limp panel can be approximated as

$$\tau \approx \left(\frac{\rho c}{\pi f \rho_m t}\right)^2 \tag{3.10}$$

where ρ_m is the mass density of the panel and t is the thickness (Wallin et al., 1999). Accordingly, the Pi number for the sound transmission through a panel (Π_m) can be expressed as

$$\Pi_m = \left(\frac{\rho c}{f \rho_m t}\right)^2 \tag{3.11}$$

Assuming that the fluid medium is air in both the full scale and scaled cases, the relationship between models can be expressed as

$$f_1 \rho_{m1} t_1 = f_2 \rho_{m2} t_2 \tag{3.12}$$

or more conveniently

$$f_1 t_1 = f_2 t_2 \tag{3.13}$$

if the same material is used for the limp panel. Hence, the frequency ratio between the full and scale models are inversely proportional to the thickness of the respective panels.

The scaling law in Equation (3.13) has a number of important limitations. First, the low frequency stiffness region is not accounted for if the panel has some compliance. Just above the low frequency stiffness region is a damping controlled region dominated by the structural resonances of the panel. These resonances are also not considered. The frequency region where the assumptions are appropriate should approximately correspond to twice the frequency of the first panel resonance. At higher frequencies, the critical frequency where structural bending and acoustic waves are equivalent to one another is not considered. Hence, the expression in Equation (3.13) is limited to the mass controlled region described earlier in Section 2.3.1.

3.2.3 Sound Propagation through a Sound Absorption Material

Sound absorbing treatments may be scaled as well. Several empirical equations exist which relate the normalized complex wave number (k_c) and characteristic impedance (Z_c) of a sound absorber to the flow resistivity(σ). These expressions are of the form

$$Z_c = \rho c(1 + C_1 X^{-C_2} - jC_3 X^{-C_4}) \tag{3.14}$$

and

$$k_c = \frac{\omega}{c}(1 + C_5 X^{-C_6} - jC_7 X^{-C_8}) \tag{3.15}$$

where C_1, C_2, C_3, C_4, C_5, C_6, C_7, and C_8 are empirically determined constants specific for a given material and $X = \rho f/\sigma$.

It follows that the scaling of the complex wave number (k_c) and characteristic impedance (Z_c) and resulting properties like the sound absorption will be valid so long as X is scaled appropriately. The Pi number (Π_2) can be expressed as

$$\Pi_2 = \frac{\rho f}{\sigma} \tag{3.16}$$

in which the flow resistivity can be expressed as

$$\sigma = \frac{R_s}{t} \tag{3.17}$$

where R_s is the flow resistance and t is the thickness of the absorber.

Assuming that the same fluid medium is used, the scaling relationship may be expressed as

$$\frac{f_1 t_1}{R_{s1}} = \frac{f_2 t_2}{R_{s2}} \tag{3.18}$$

where the numerators are consistent with Eqn. (3.13). That implies that the flow resistances for the materials should be equivalent (i.e., $R_{s1} \approx R_{s2}$). If it can be assumed that the flow resistance is proportional to the material density, the flow resistance will remain constant if the material is compressed by the scaled amount.

This is a rough approximate that suffices in some cases (Ruan and Herrin, 2017) at least to engineering accuracy.

3.3 Summary

This chapter provides a review of developing some basic scale modeling laws as detailed by Emori and Schuring (1977). Scaling rules for sound propagation in air, through a membrane, and through a sound absorbing material have been described. For a membrane and sound absorbing material, the scaling rules are engineering approximations.

Copyright © Nan Zhang 2018

CHAPTER 4 EXAMPLE – BARRIER

4.1 Barrier Insertion Loss

Scale modeling was applied to a simple barrier problem. A photograph of the full-scale and scaled barrier is shown in Figure 4.1. Both barriers are made of medium-density fiberboards (MDF). The smaller barrier is 0.61 m × 0.61 m square and the larger barrier is two times the scale. The thicknesses of the large and small barriers are 19 mm and 9.5 mm respectively. A point monopole source is placed on one side of the barrier. The monopole source was developed in prior work (Liu et al., 2011). A shop air supply is attached through a throat into a whiffle ball that is taped at the top forcing the air through the side holes. The source has been shown to properly represent a monopole.

Figure 4.1 Photograph of full-scale and scaled barriers

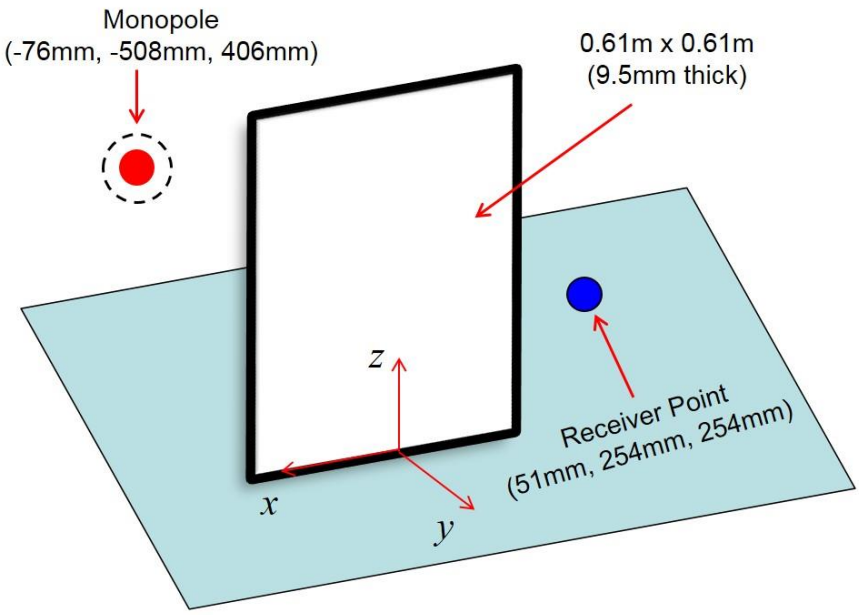

Figure 4.2 Schematic showing of the barrier insertion loss test

The schematic of the barrier insertion loss test is shown in Figure 4.2. For the smaller barrier, the source was located 508 mm from the barrier, 406 mm off the ground and 76 mm off the horizontal center of the panel. The measured receiver point is in the shadow zone of the barrier and is located 254 mm away from the barrier, 254 mm off the ground, and 51 mm off the center line.

Figure 4.3 Measurement setup for full barrier and its scale model

The measurement setup picture for the full barrier and scale model is shown in Figure 4.3. The FEM model with AML boundary condition is shown in Figure 4.4.

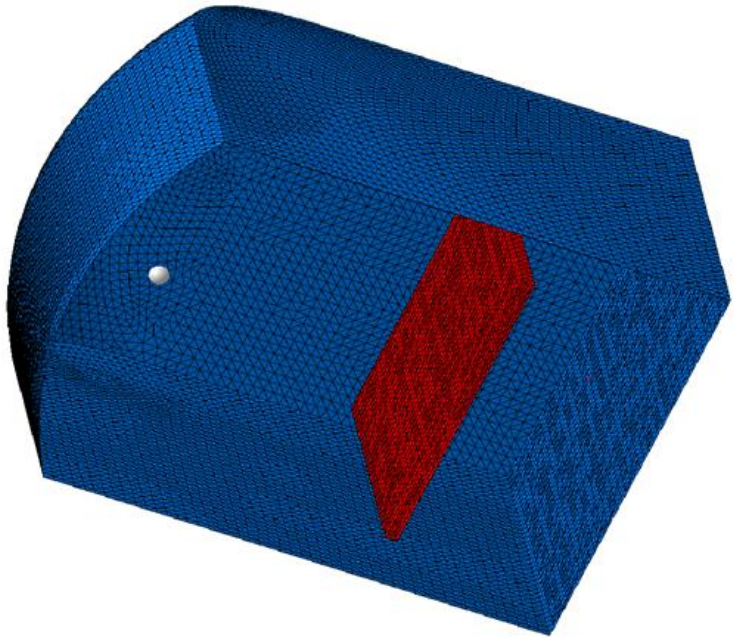

Figure 4.4 FEM model of the barrier

Insertion loss, which is commonly used to index effectiveness of barriers, is defined as

$$IL = L_p - L_{p_{wb}} \tag{4.1}$$

where L_p and $L_{p_{wb}}$ are the sound pressure level without and with the barrier in dB, respectively. An insertion loss comparison between the unscaled and scaled models is shown in Figure 4.5.

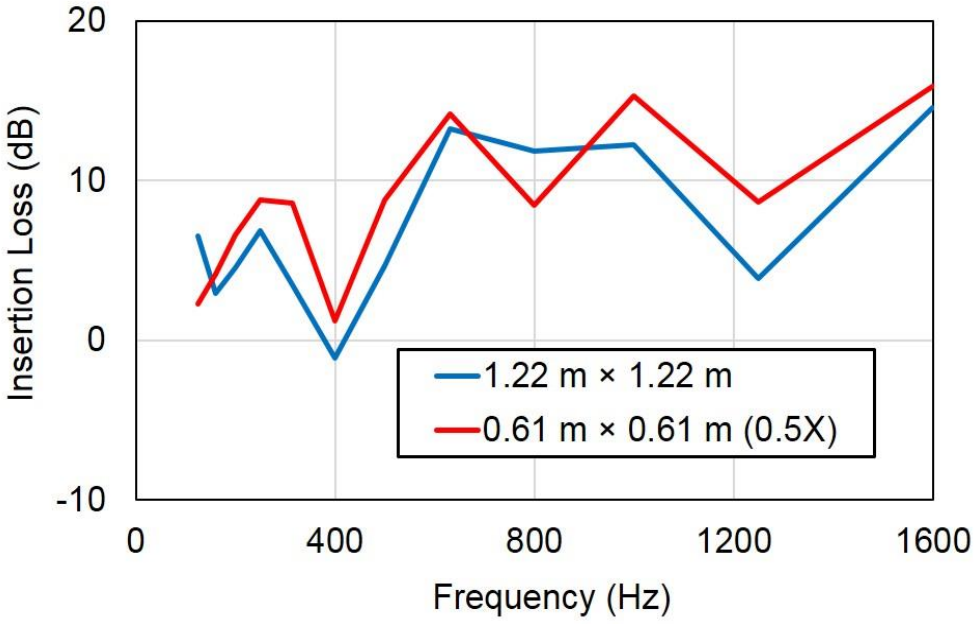

Figure 4.5 Insertion loss comparison for barrier between full and scale model

It can be seen that the results generally agree with each other. Differences most likely arise due to the source not behaving like a monopole for the smaller barrier. Results compared to the textbook calculation of Long (2014) and acoustic finite element simulation using the Siemens Virtual.Lab (2015) software are shown in Figure 4.6. Similar trends can be observed between FEM simulation and measurement though there are significant differences at individual frequencies. Results demonstrate the applicability of using scale models for barrier problems. However, it will likely prove difficult to properly scale the acoustic source.

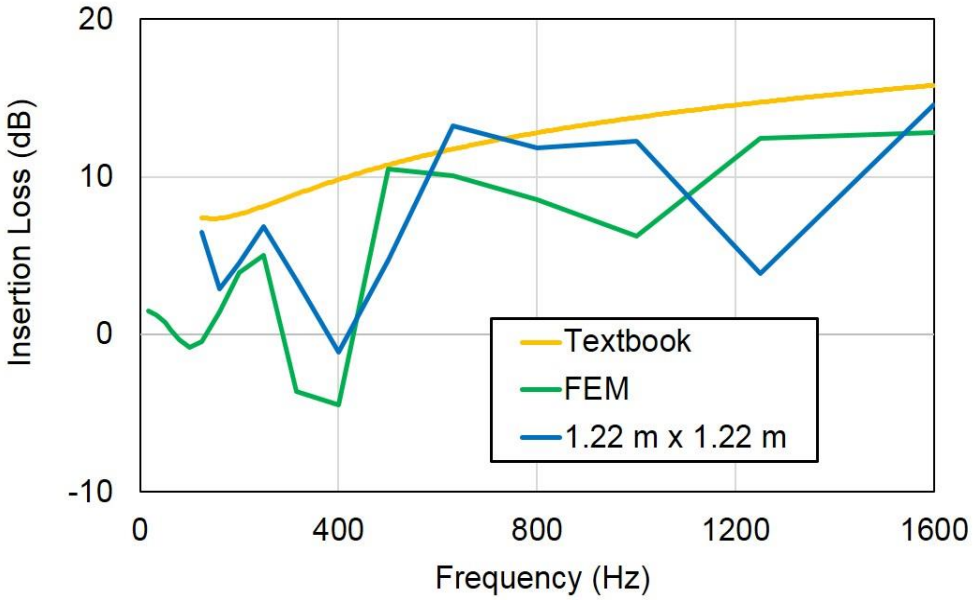

Figure 4.6 Analytical, FEM and test results comparison for barrier

4.2 Summary

The first test case considered was for rectangular barrier. Insertion loss was compared between a full-scale and 2X scale model with reasonable agreement. There are some minor differences that can likely be explained by the source itself not being scaled properly in the scale model.

Copyright © Nan Zhang 2018

CHAPTER 5 EXAMPLE – PARALLEL TUBES

5.1 Transmission Loss through Parallel Tubes

A second test case featured 9 relatively long parallel tubes drilled into ABS plastic and positioned in a transmission loss test rig as shown in Figure 5.1. Both the baseline and 2.85× scale model case are made from the same material, and the transmission loss is measured in appropriate sized test rigs using the two-load method according to ASTM E2611 (ASTM, 2009). The baseline case is a 34.9 mm diameter cylinder that is 107 mm in length with 9 holes of diameter 4.0 mm. The scale model is 2.85 times the baseline.

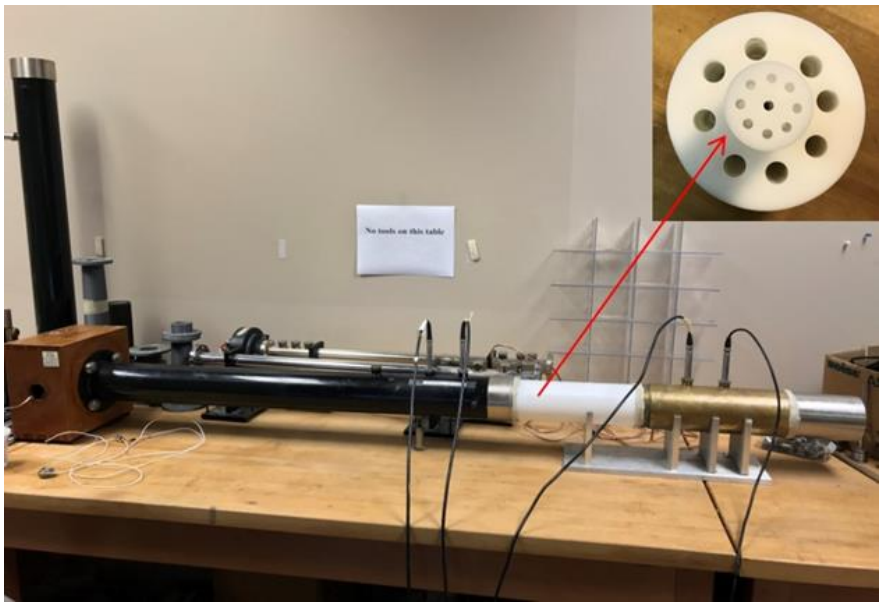

Figure 5.1 Transmission loss test setup for an array of parallel tubes

A plane wave model was also developed using SIDLAB (SIDLAB 4.1.0, 2017). For long tubules, it can be anticipated that viscous losses may be important.

According to Keefe (Keefe, 1984), the complex air density (ρ) and speed of sound (c) in a small cylindrical duct can be expressed as

$$\rho = \frac{\rho_0}{1 - F(s)} \tag{5.1}$$

and

$$c = c_0 \frac{\left(1 - F(s)\right)^{1/2}}{\left[1 + (\gamma - 1)F\left(\sqrt{\nu}s\right)\right]^{1/2}} \tag{5.2}$$

where γ is specific heat ratio and ν is Prandtl number. s is the dimensionless ratio of duct radius (a) to the viscous boundary-layer thickness. It is expressed as

$$s = \frac{a}{\sqrt{\eta/\rho_0\omega}} \tag{5.3}$$

where η is the shear viscosity coefficient and $F(s)$ is defined in terms of the Bessel functions $J_0(x)$ and $J_1(x)$ as

$$F(s) = \frac{2}{\sqrt{-j}s} \frac{J_1\left(\sqrt{-j}s\right)}{J_0\left(\sqrt{-j}s\right)} \tag{5.4}$$

Using Eqns. (5.1-5.4), thermo-viscous dissipation is included in the plane wave model. The Prandtl number (ν) is specified as 0.8, the specific heat ratio γ is 1.4, and the shear viscosity coefficient (η) of air is 1.64E-5 m^2/s at 1 bar and 40°C.

The transmission loss is compared between the baseline and 2.85× scale model in Figure 5.2 with good agreement. Plane wave simulation is included for comparison.

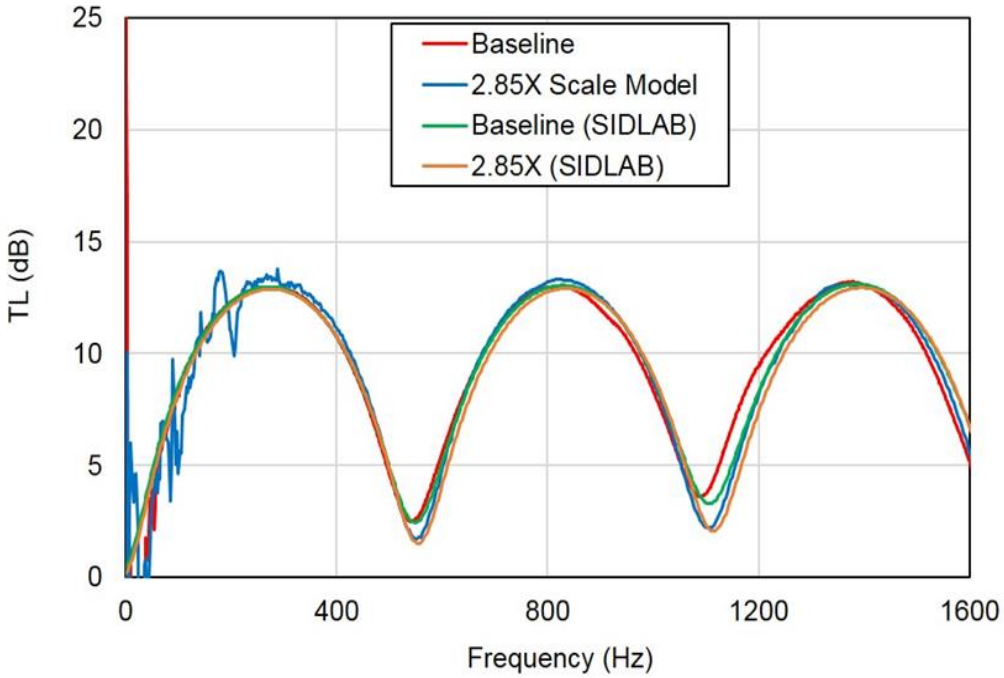

Figure 5.2 Transmission loss results comparison

Notice that viscous losses are slightly higher for the baseline case due to the smaller tube diameter. This is evident in the transmission loss troughs at ~550 Hz and ~1090 Hz. This can be seen in the plane wave simulation as well. Note that the effect is only about 1 dB. These results do indicate that viscous effects may be quite important if the baseline (i.e., smaller) case has very small dimensions which will likely be the case for some small electronics devices. However, this effect can likely be estimated and adjusted for in the scale model.

5.2 Summary

The transmission loss through nine parallel tubes was determined using a 2.85X scale model. Results were in close agreement with the unscaled case though there was some evidence of thermo-viscous effects at the troughs and peaks of transmission loss. The results lend credibility to the use of scale models for small electronics equipment.

Copyright © Nan Zhang 2018

CHAPTER 6 EXAMPLE – CUBOID WITH CYLINDRICAL WELL

6.1 Introduction

Most scale modeling research has been aimed at architectural applications where the scale model is much smaller than the actual acoustic space. However, it can be observed that scale models may also be applied to model small spaces where instrumenting the system is problematic. In this chapter, the emphasis is shifted to looking at the feasibility of using scale models for small systems.

Acoustics is a major issue in information technology equipment. Obvious applications include handheld devices like cell phones, tablets, and medical devices. In these applications, measurement grade microphones are too large to be placed inside the equipment, so it is difficult to make measurements in the interior of the equipment due to the small size. The current work looks at scale model feasibility for these and other applications. For example, the microphones and speakers in cellphones are placed in small wells and are covered by membranes or absorbers. The geometry of the well and membrane or absorber affect the acoustics.

Presently, numerical acoustics is relied upon but there is little in the way of model validation. By increasing the size of the geometry, configurations can be studied and modified, and simulation models can be validated. The objective of this work is also to validate that scale models of increased size can be effectively used but also to highlight some of the potential limitations.

In this chapter, scale modeling is applied to a more challenging example. A point source is placed above a structure with a cylindrical duct bored into it. A transfer function is measured between positions outside and inside of the duct for both the full and 5.7× scale model. The geometry is modified by a) erecting a cylindrical barrier around the opening, b) by placing a panel over the opening and c) by positioning a porous sound absorber over the opening. Full-scale and scale models are compared in each case.

6.2 Test Description

Scale modeling was applied to a box-like structure with a cylindrical well. A photograph of the structure and 5.7× scale model is shown in Figure 6.1 on the left. The box is 0.1 m × 0.1 m × 0.15 m and the monopole source is positioned as shown in the figure (the origin of the coordinate system is located at the bottom center of the test object). A dimensioned view of the well is shown in Figure 6.1 on the right. The diameter of the cylinder at the top of the well is 60 mm whereas the diameter of the deeper cylinder is 20 mm. The depth of the well is 70 mm.

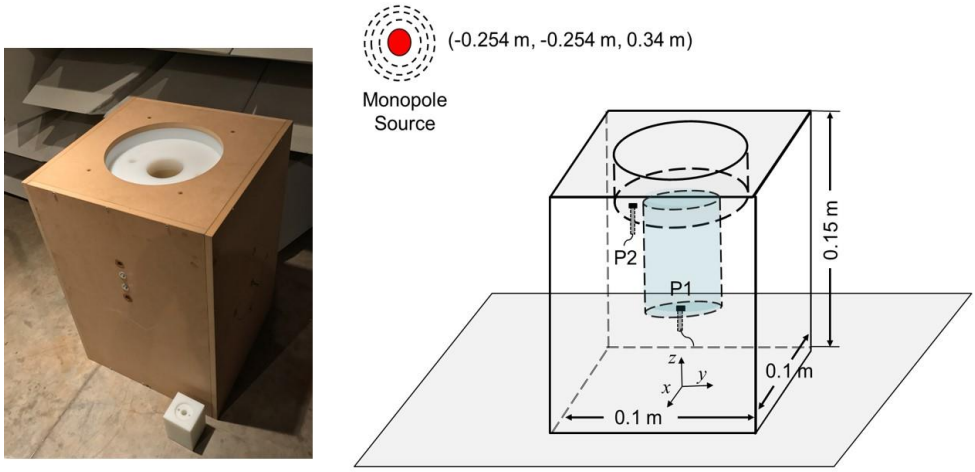

Figure 6.1 Photograph of full structure and its scale model (left). Schematic dimensions for the full model (right)

Microphones were positioned at the locations as shown in Figure 6.1 where P2 is 20 mm off the center of the top opening and P1 is at the bottom center of the well. The transfer function between microphones 1 and 2 was measured and compared. The transfer function measurement setup for the unscaled (i.e., small) case is shown in Figure 6.2, and the 5.7X scale model is shown in Figure 6.3.

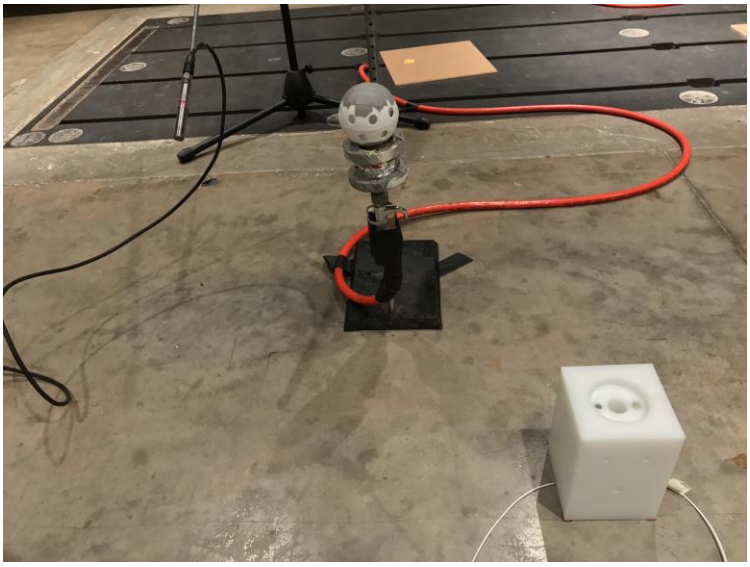

Figure 6.2 Transfer function measurement setup for full model

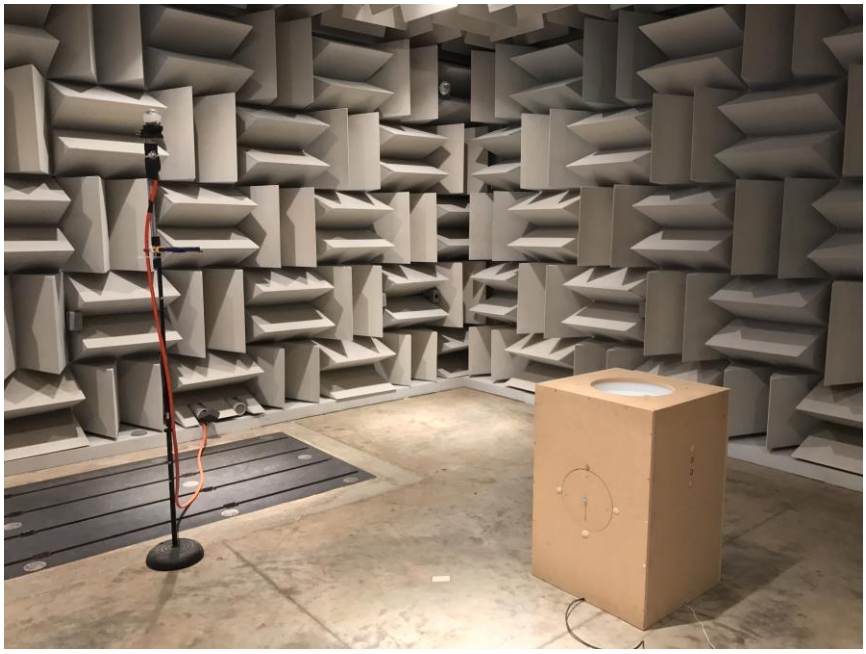

Figure 6.3 Transfer function measurement setup for scale model

The FEM model for full structure with AML boundary condition in LMS Virtual.Lab (2015) is shown in Figure 6.4. The model consisted of 68,205 nodes and 328,364 linear tetrahedral elements.

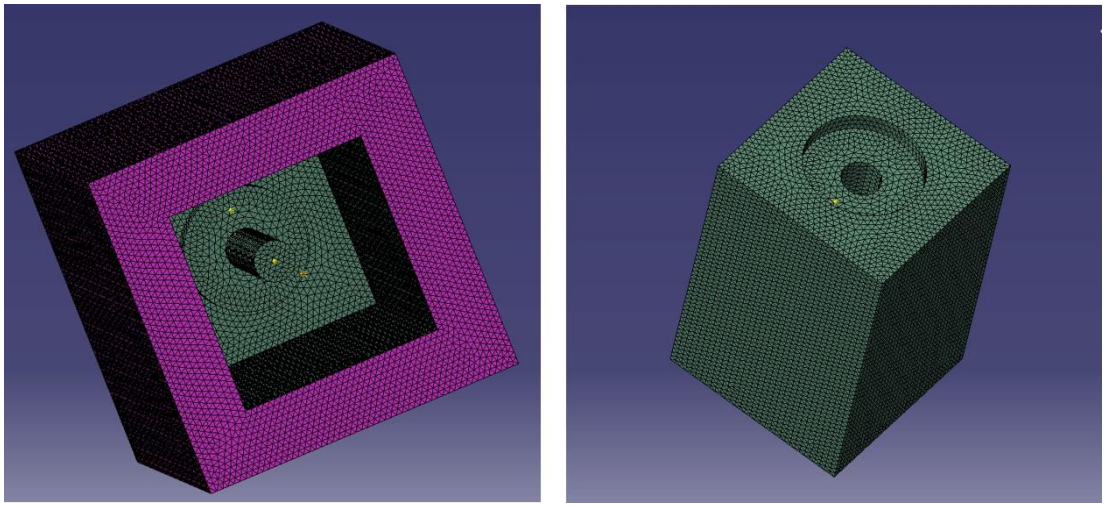

Figure 6.4 Finite and boundary element models

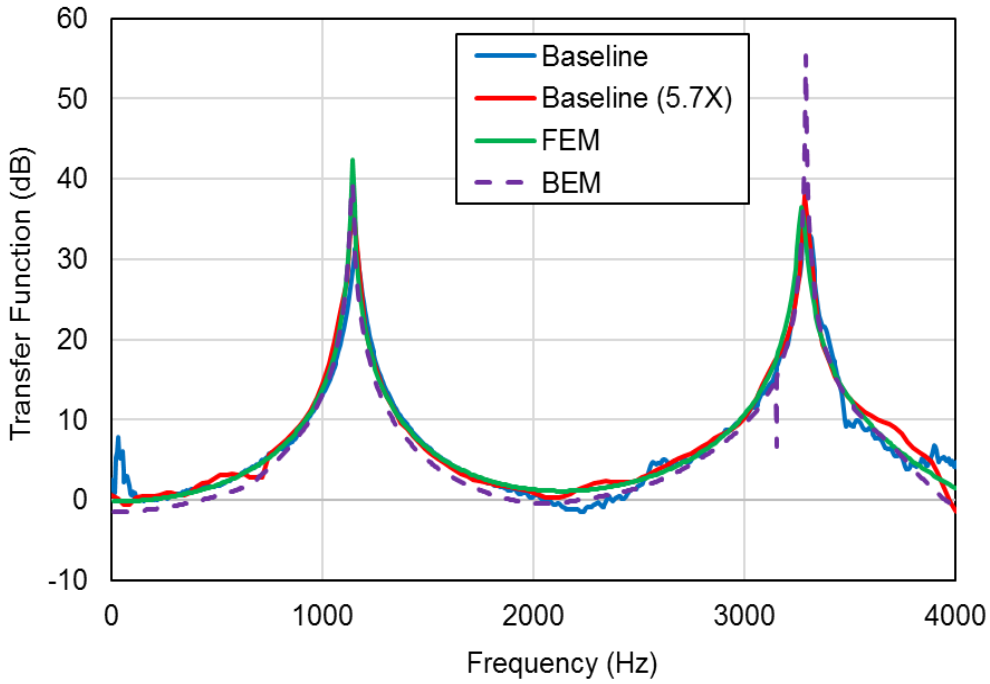

Figure 6.5 Transfer function comparison showing unscaled, 5.7X scale, and FEM and BEM simulation.

Transfer function comparisons between the baseline test object and the scale model are shown in Figure 6.5. There are obvious resonances at $\frac{1}{4}c/d$ and $\frac{3}{4}c/d$ frequencies which are approximately 1140 Hz and 3314 Hz, where c is the speed of sound and d is the depth of the well. Scale model results also demonstrate acceptable correlation with numerical simulation (FEM and BEM).

6.3 Modification Cases

6.3.1 Cylindrical Barrier Treatment

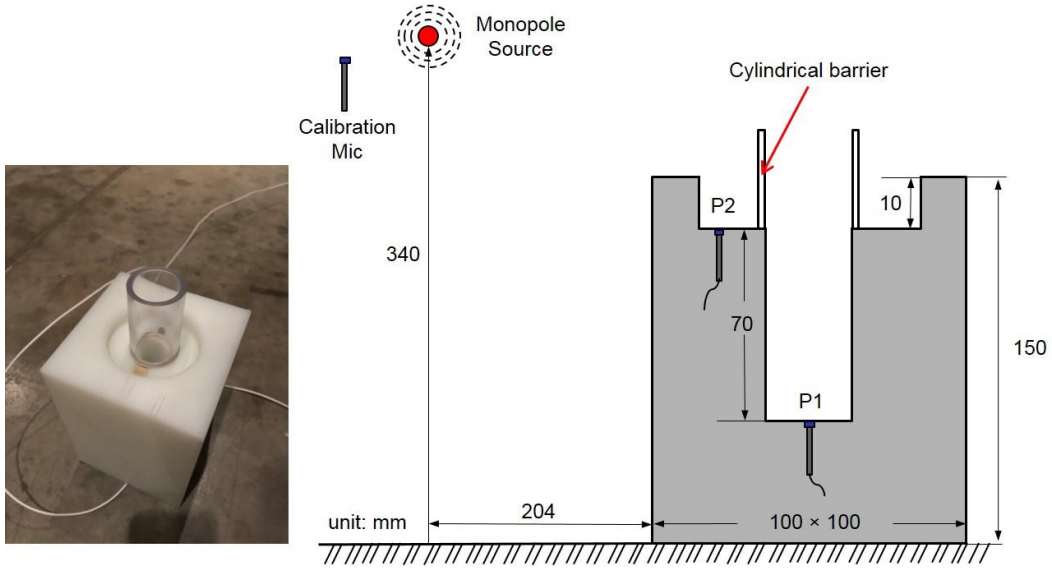

Figure 6.6 Photograph of the cylindrical barrier treatment for full structure (left) with the schematic dimensional view

A cylindrical barrier erected around the well is shown in Figure 6.6. The length of the barrier is 38.1 mm and has the same diameter as the well. The barrier is made of UHMW Polyethylene plastic. The thickness of the wall is 19 mm. Superglue is used to attach the barrier on the structure and putty is used for sealing.

For the 5.7X scale model, the same material is used for the barrier. However, the thickness of the barrier remains the same in the scale model and so is not scaled. A schematic showing the FEM modeling approach is shown in Figure 6.7.

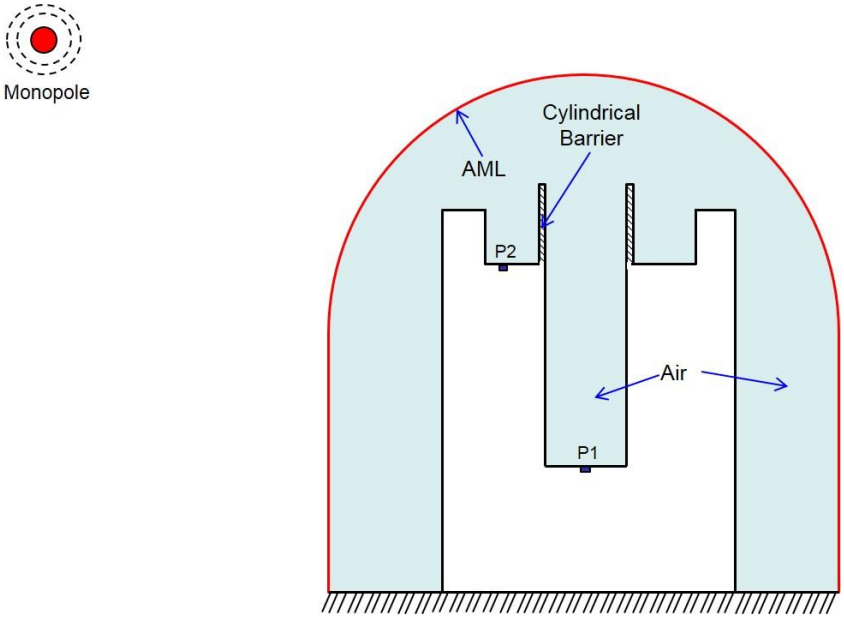

Figure 6.7 Schematic view of the FEA model for cylindrical barrier treatment

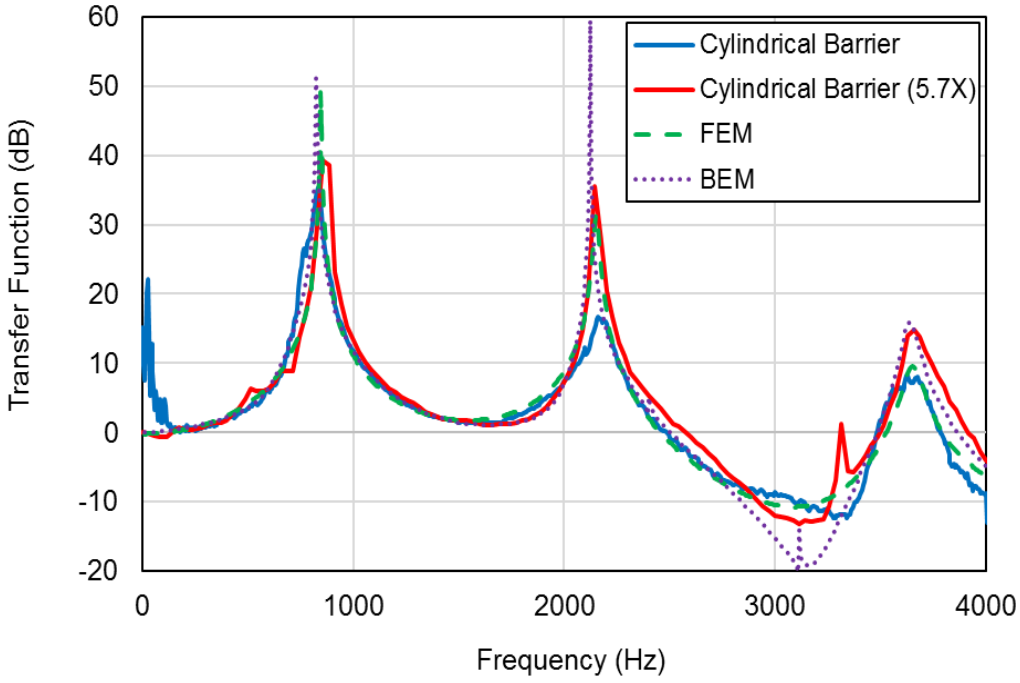

Figure 6.8 Transfer function comparisons between measured, and FEM and BEM simulation.

Scale and unscaled measurement results are compared in Figure 6.8. FEM and BEM numerical simulation results are also included. It can be observed that the scale model results faithfully represent the trends but transfer functions are lower at the resonances and higher at the anti-resonances due to greater viscous friction in the smaller test object. Scaled and unscaled results with the cylindrical barrier included are shown as well. The cylindrical barrier adds to the length of the cylindrical well and moves the quarter wave frequencies lower in frequency. The scale model correctly captures the resonant frequencies.

6.3.2 Membrane Treatment

A panel is placed over the circular opening. The panel is made from UHMW polyethylene with a density of 930 $\mathrm{kg/m^3}$. The panel was attached using double sided tape. A photo of the treatment is shown in Figure 6.9.

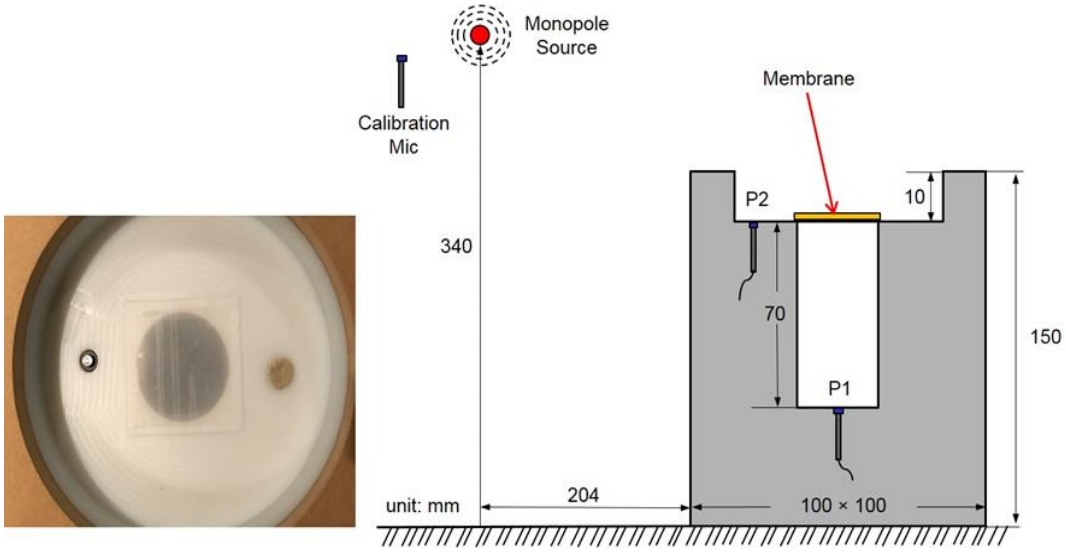

Figure 6.9 Photograph of the membrane treatment for scale model structure (left) with the schematic and dimensions (right)

Figure 6.10 shows transfer function results when a panel barrier is placed over the opening. As anticipated, the resonant frequencies are reduced. However, it is interesting that compliance effects of the panel seem to be unimportant. This is evidenced by the fact that the resonant frequencies are not all that different between the unscaled and scaled models. Apparently, the double sided tape can be used to approximate limp body motion of the panel. Notice that the acoustic resonances are significantly decreased using the panel barrier. It can also be observed that the transfer function decreases in amplitude.

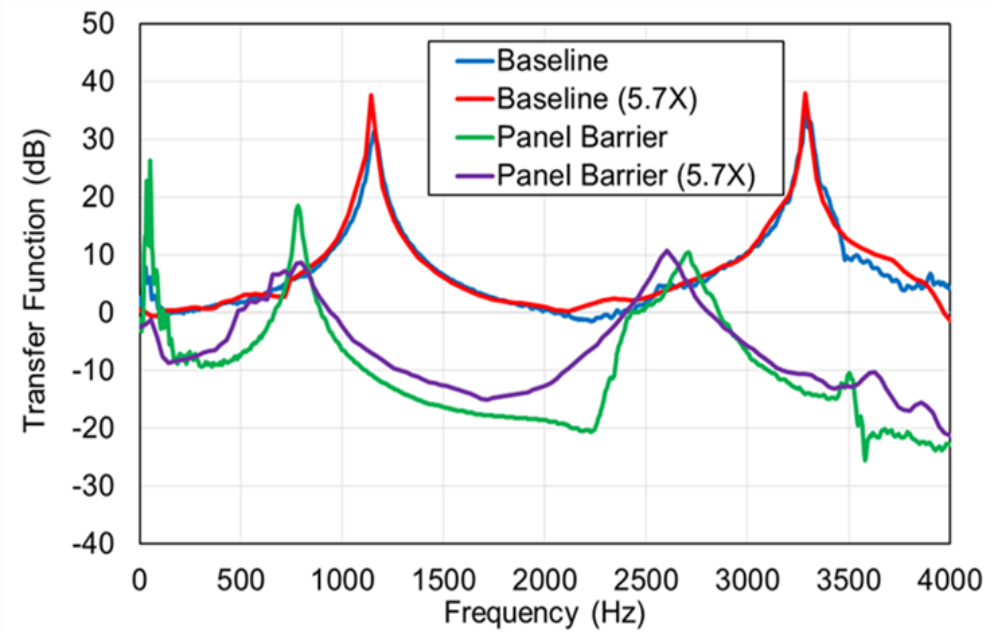

Figure 6.10 Transfer function comparison between baseline and membrane treated. Scale model results are also included

6.3.3 Absorption Treatment

Polyurethane foam was placed at the entrance to the opening. For the unscaled (smaller) case, the material was compressed to a thickness of 15 mm. For the 5.7× scale model, the material was uncompressed and had a thickness of 86 mm. As a rough approximation, it was assumed that the flow resistivity would increase as it was compressed according to the scaling factor. A wire mesh was used to compress the material on each side. This assumption will be material dependent and should be checked in each case. In this case, the flow resistance was measured using a standard airflow resistance measurement according to ASTM C522 (ASTM, 2003) and was 366 and 338 rayls for the full-scale and 5.7× scale, respectively. A photograph of the sound absorptive treatment is shown in Figure 6.11 on the left. Transfer functions were measured for both full and scale

models. Quarter inch and half inch microphones were used for the full-scale and 5.7× models respectively.

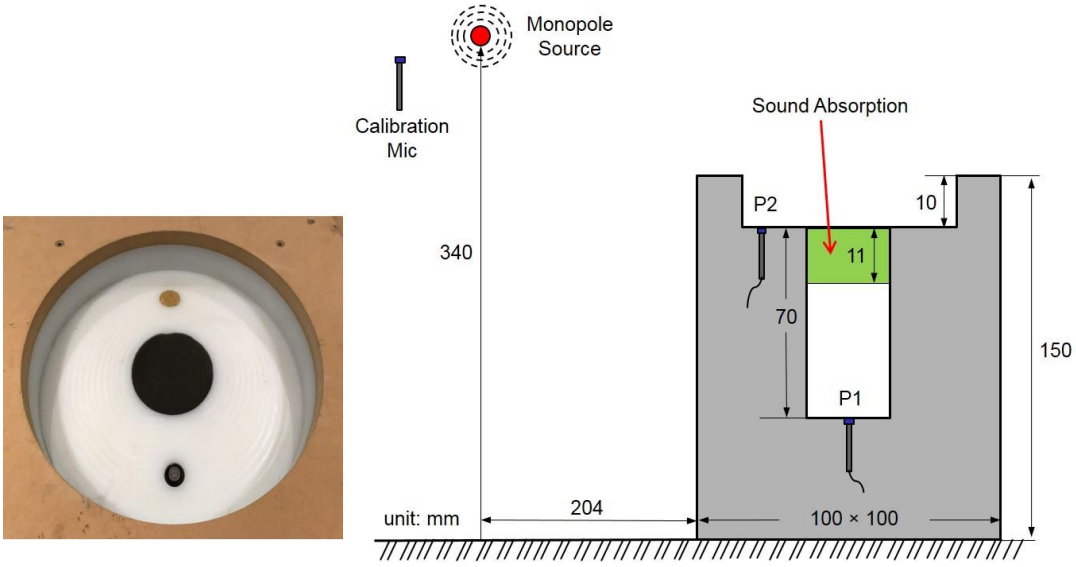

Figure 6.11 Photograph of the absorption treatment for scale model structure (left) with the schematic dimensional view

A finite element simulation model was also prepared for both the cases with sound absorption using the Siemens Virtual.Lab software (Siemens, 2015). Figure 6.12 is a schematic of the modeling approach. The FEM simulation model had 7,019 nodes and 29,526 elements. A perfectly matched layer boundary condition is used to simulate the radiating boundary. The implementation in Siemens Virtual.Lab adjusts the thickness and refinement of the layer as a function of frequency automatically and is referred to as an automatically matched layer. The point source is modeled as a monopole source. The sound absorption is modeled using the Johnson-Champoux-Allard (Allard, 1993) model in Siemens Virtual.Lab. The measured flow resistivity of 23,058 rayls/m is used. A porosity of 0.96 and tortuosity of 1.24 is assumed for the polyurethane foam.

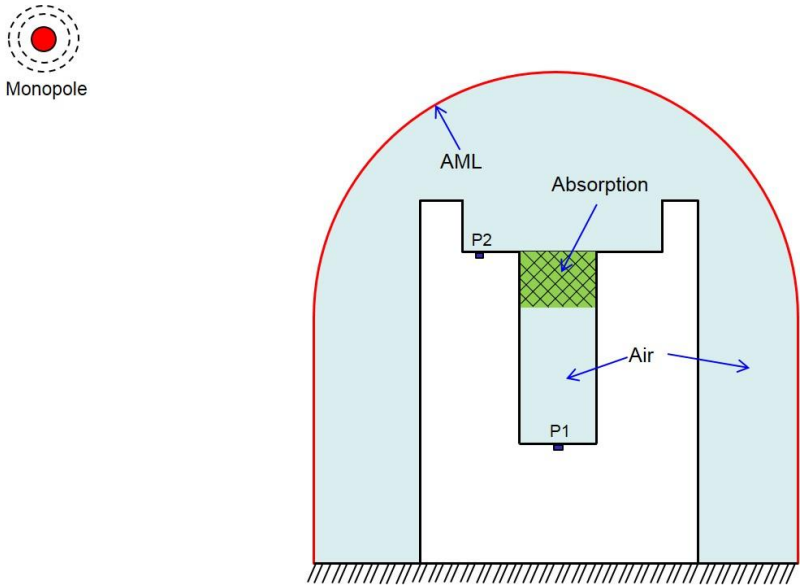

Figure 6.12 Schematic view of the FEA model for absorption treatment

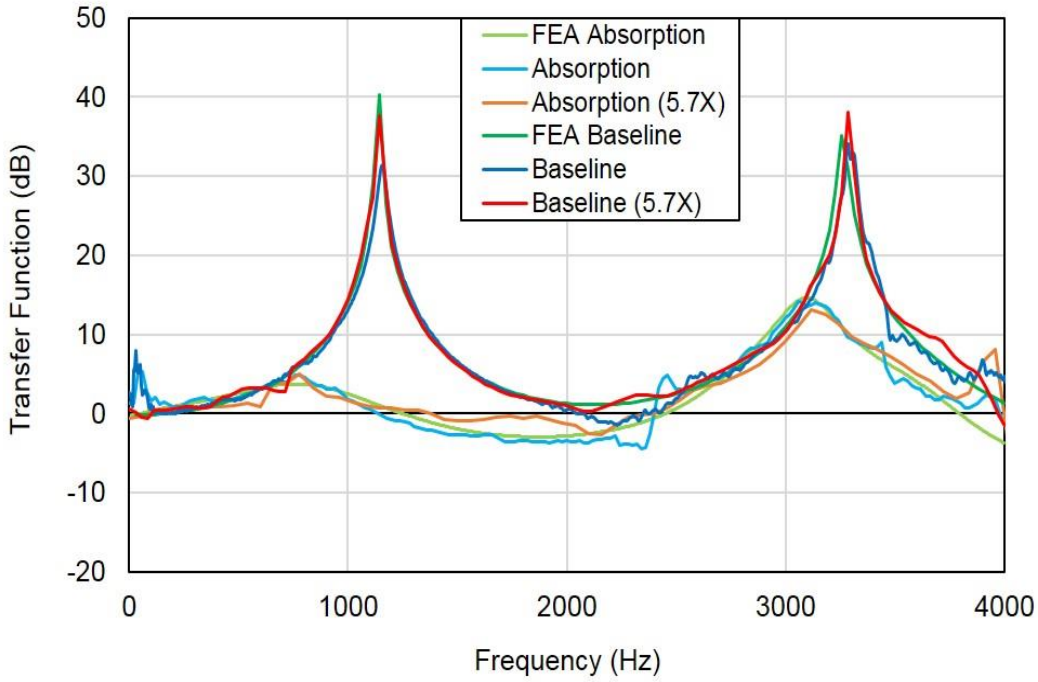

Figure 6.13 FEM and experiment results of the transfer function comparison for the absorption treatment with scale model

The transfer function P_2/P_1 was measured and results are shown in Figure 6.13. Measured results are compared for the full and 5.7 × scale model. Simulation results are also included for comparison. For the baseline case without sound absorption, resonances are evident at frequencies corresponding to $1/4\,c/d$ and $3/4\,c/d$. In addition, it can be observed that after adding the sound absorption treatment, the peaks at resonance are greatly reduced and are shifted lower in frequency as anticipated. The results show that the scale model can be used to predict the impact of adding sound absorption. It also can be seen that this case could be easily simulated. Moreover, it illustrates that a 5.7× scale model could be used to validate the simulation model.

6.4 Summary

Scale modeling rules have been reviewed for acoustic propagation and transmission through membranes and sound absorbing materials. Examples considered included a test object with cylindrical well covered by cylindrical barrier, membrane, and sound absorption. Good agreement between the prototype and scale model was noted in each case. In addition, results compared well with numerical simulation models. Test results have shown that scale models can be used to reliably identify resonances and trends. However, amplitudes may not compare well due to higher damping when objects are small.

Copyright © Nan Zhang 2018

CHAPTER 7 CONCLUSIONS AND FUTURE RECOMMENDATIONS

7.1 Conclusions

The objective of this thesis was to conduct initial exploratory studies on the viability of using scale models to investigate the sound fields around small electronic devices. Measurements are challenging in these situations due to the small geometry. However, it is proposed that scale models can be constructed that are much larger in size and easier to instrument.

Scaling laws were reviewed and detailed for acoustic wave propagation, sound transmission through panels and membranes, and sound absorbing materials. It was shown that a weaker form of scaling was used for membranes and sound absorbing materials.

Scale models were then applied to three examples. In each case, the scale model was also compared to finite element simulation. In the first example, a simple rectangular barrier was examined with a point source on one side and a microphone in the shadow region. Results correlated reasonably well though the results appear to be very sensitive to the location of microphone and possibly the thickness of the barrier. Differences between the unscaled and scaled models were on the order of 3-5 dB.

The second example is an array of 9 parallel tubes. The transmission loss was determined in an impedance tube. Correlation was very good between the unscaled and scaled models. It was noted that the thermo-viscous effects can

become important if the original geometry is very small in size. This should be borne in mind when looking at the results.

The final example was a rectangular cuboid with cylindrical well. The height of the cuboid was 15 cm and the diameter of the well was 20 mm. This was the smallest size that could be instrumented using the available equipment in the University of Kentucky Vibro-Acoustics Laboratory. The scale model was 5.7 times larger. Transfer functions between two measurement locations (at the top and one at the bottom of the well) were compared between the unscaled and scaled models. This was repeated with 1) a cylindrical barrier around the well, 2) a thin membrane covering the well opening, and 3) a sound absorptive layer covering the well opening. Correlation between unscaled and scaled models were good in each case. However, the scale model did not adequately model bending modes in the membrane and thermo-viscous or damping effects in the unscaled case.

7.2 Recommendations for Future Work

The following recommendations are suggested for future research efforts.

1) It would be helpful to explore thermo-viscous effects on even smaller geometries than those studied. This would require smaller instrumentation than what is currently available at the University of Kentucky Vibro-Acoustic Laboratory.
2) Sound absorption was scaled by simply compressing the material. Rules for when this simple scaling procedure is appropriate should be developed.
3) More difficult cases that combine several features should be considered.

Copyright © Nan Zhang 2018

REFERENCES

J. F. Allard, (1993). *Propagation of Sound in Porous Media: Modelling Sound Absorbing Materials*, Elsevier Applied Science, London and New York.

ASTM Standard, C522, (2003). “Standard Test Method for Airflow Resistance of Acoustical Materials.”

ASTM Standard, E2611, (2009). “Standard Test Method for Measurement of Normal Incidence Sound Transmission of Acoustical Materials based on Transfer Matrix Method.”

R. L. Bannister, (1968). “Comparison of the dynamic response of a complex plastic model with its prototype,” The Journal of the Acoustical Society of America, 43(6), 1306-1310.

R. L. Bannister, (1975). “Structural models for vibration control,” Noise Control Engineering Journal, 4(2), 84-92.

S. Brown, (2016). “The suitability of additive manufacturing materials in a 1:10 scale reverberation chamber,” Proceedings of Inter-Noise 2016, Hamburg, Germany.

T. Busch, M. Hodgson and C. Wakefield, (2003). “Scale-model study of the effectiveness of highway noise barriers,” The Journal of the Acoustical Society of America, 114(4), 1947-1954.

G. Cheng and D. W. Herrin, (2015). “Prediction of generator set noise in the far field using panel contribution analysis and scale modeling,” 22nd International Congress of Sound and Vibration Proceedings, Florence, Italy.

G. Cheng and D. W. Herrin, (2018). “Application of panel contribution analysis combined with scale modeling to predict sound pressure levels in a bakery,” Proceedings of Inter-Noise 2018, Chicago, USA.

B. Day and R. J. White, (1969). “A study of the acoustic field in landscaped offices with the aid of a tenth-scale model,” Applied Acoustics, 2(3), 161-183.

R. I. Emori and D. J. Schuring, (1977). *Scale Models in Engineering: Fundamentals and Applications,* Pergamon Press, Oxford.

D. W. Herrin, T. W. Wu and A. F. Seybert, (2003). “Practical issues regarding the use of the finite and boundary element methods for acoustics,” Building Acoustics, 10(4), 257-279.

D. W. Herrin, G. Cheng, S. C. Campbell, J. M. Stencel, (2017). “Noise reduction on a jumbo drill using panel contribution analysis and scale modeling,” Proceedings of Inter-Noise 2017, Hong Kong, China.

K. V. Horoshenkov and D. C. Hothersall, (1996). “Porous materials for scale model experiments in outdoor sound propagation,” Journal of Sound and Vibration, 194(5), 685-708.

K. U. Ingard and T. A. Dear, (1985). “Measurement of acoustic flow resistance,” Journal of Sound and Vibration, Vol. 103, pp. 567-572.

ISO 140-4, (1998). “Acoustics - Measurement of sound insulation in buildings and of building elements – Part 4: Field measurements of airborne sound insulation between rooms.”

ISO 3382, (1997). “Acoustics – Measurement of the reveration time of rooms with reference to other acoustic parameters.”

E. S. Ivey and G. A. Russell, (1977). “Acoustical scale model study of the attenuation of sound by wide barriers,” J. Acoust Soc. Am. 62(3), 601-606.

J. Y. Jeon, J. W. Ryu, Y. H. Kim, S. Sato, (2009). “Influence of absorption properties of materials on the accuracy of simulated acoustical measures in 1:10 scale model test,” Applied Acoustics, 70(4), 615-625.

A. Jolibois, J. Defrance, H. Koreneff, P. Jean, D. Duhamel, V.W. Sparrow, (2015). “In situ measurement of the acoustic performance of a full scale tramway low height noise barrier prototype,” Applied Acoustics, 94, 57-68.

V. L. Jordan, (1970). “Acoustical criteria for auditoriums and their relation to model techniques,” J. Acoust Soc. Am. 47(2A), 408-412.

V. L. Jordan, (1975). “Auditoria acoustics: Development in recent years,” Applied Acoustics, 8(3), 217-235.

D. W. Kahn and J. Tichy, (1986). “An investigation of the sound field above the audience in large lecture halls with a scale model,” The Journal of the Acoustical Society of America, 80(3), 815-827.

D. H. Keefe, (1984). “Acoustic wave propagation in cylindrical ducts: transmission line parameter approximations for isothermal and nonisothermal boundary conditions,” J. Acoust. Soc. Am. 75(1), 58-62.

Y. W. Lam and S. C. Roberts, (1992). “A simple method for accurate prediction of finite barrier insertion loss,” J. Acoust. Soc. Am. 93(3), 1445-1452.

Y. W. Lam, (1994). “Using Maekawa’s chart to calculate finite length barrier insertion loss,” Applied Acoustics, 42(1), 29-40.

A. Leblanc and A. Lavie, (2017). “Three-dimensional-printed membrane-type acoustic metamaterial for low frequency sound attenuation,” J. Acoust. Soc. Am. 141(6), 538-542.

Xianhui Li, (2013). “A scaling approach for high-frequency vibration analysis of line-coupled plates,” Journal of Sound and Vibration, 332(18), 4054-4058.

J. Liu, L. Zhou and D. W. Herrin, (2011). “Demonstration of vibro-acoustic reciprocity including scale modeling,” SAE Noise and Vibration Conference, Paper No. 2011-01-1721.

M. Long, (2014). *Architectural Acoustics 2nd Edition*, Academic Press, Waltham, MA.

Z. Maekawa, (1968). “Noise reduction by screens,” Applied Acoustics, 1(3), 157-173.

A. Muradali and K.R. Fyfe, (1998). “A study of 2D and 3D barrier insertion loss using improved diffraction-based methods,” Applied Acoustics, 53(1-3), 49-75.

C. J. Naify, C. M. Chang, G. Mcknight, S. R. Nutt, (2012). “Scaling of membrane-type locally resonant acoustic metamaterial arrays,” J. Acoust. Soc. Am. 132(4), 2784-2792.

A. Nilsson and B. Liu, (2012). *Vibro-Acoustics, Volume* 1, Science Press, Beijing.

S. Oerlemans and P. Sijtsma, (2004). “Acoustic array measurements of a 1:10.6 scaled airbus A340 model,” Proceedings of 10th AIAA/CEAS Aeroacoustics Conference, Manchester, Great Britain.

R. J. Orlowski, (1990). “Scale modelling for predicting noise propagation in factories,” Applied Acoustics, 31(1-3), 147-171.

R. J. Orlowski, (1984). “The arrangement of sound absorbers for noise reduction-Results of model experiments at 1:16 scale,” Noise Control Engineering Journal, 22(2), 54-60.

J. H. Rindel, (2011). “Room acoustic modelling techniques: A comparison of a scale model and a computer model for a new opera theatre,” Building Acoustics, 18(3-4), 259-280.

K. Ruan and D. W. Herrin, (2017). “Using scale modeling to assess heating and air conditioning duct attenuation,” Proceedings of Inter-Noise 2017, Hong Kong, China.

J. K. Ryu and J. Y. Jeon, (2008). “Subjective and objective evaluations of a scattered sound field in a scale model opera house,” J. Acoust. Soc. Am. 124(3), 1538-1549.

K. Saito and K. Kuwana, (2017). “Scale modeling vibro-acoustics,” Acoust. Sci & Tech. 38(3), 113-119.

Siemens, (2015). LMS Virtual.Lab Online Help. Munich, Germany.

SIDLAB 4.1.0, (2017). Acoustics User Manual and Online Help.

N. N. Voronina, (1985). “Scale modeling of the acoustical characteristics of layers of fibrous sound absorbing materials,” Soviet Physics-Acoustics, 31, 402-404.

G. J. Wadsworth and J. P. Chambers, (2000). “Scale model experiments on the insertion loss of wide and double barriers,” The Journal of the Acoustical Society of America, 107(5), 2344-2350.

H. P. Wallin, U. Carlsson, M. Abom, H. Boden and R. Glav, (1999). *Sound and Vibration,* KTH, Stockholm.

VITA

Nan Zhang was born in Hohhot, China in 1989. He graduated from Hohhot No.2 Middle School in 2008. He received his Bachelor's Degree of Science in Automotive Engineering from Xi'an University of Technology, China in 2012. On August 2014, he enrolled in master program in Mechanical Engineering at University of Kentucky. During his four years graduate study, he published a conference proceeding at 2017 Noise-Con conference as first author, and was rewarded Hallberg Foundation Award and Best Student Paper Competition Award by Institute of Noise Control Engineering (INCE). He then published the second conference proceeding as first author at 2018 Inter-Noise conference, and received Michiko So Finegold Travel Award by INCE-USA.

Nan Zhang